268258

EXTREMELY BROAD BAND FERRITE DEVICES

by: David S. Friedman and Jerome Rosen

Prepared for

ELECTRONICS RESEARCH DIRECTORATE
AIR FORCE CAMBRIDGE RESEARCH LABORATORIES
OFFICE OF AEROSPACE RESEARCH
UNITED STATES AIR FORCE
BEDFORD, MASSACHUSETTS

ASTIA

565 500

Merrimac

RESEARCH AND DEVELOPMENT. INC.

517 LYONS AVE. — IRVINGTON, N. J.

EXTREMELY BROAD BAND FERRITE DEVICES

by: David S. Friedman and Jerome Rosen

Merrimac Research and Development, Inc.

517 Lyons Avenue, Irvington 11, New Jersey

FINAL REPORT

Report No. E-41-5

Contract AF-19-(604)-7288

September 5, 1961

Prepared
for

ELECTRONICS RESEARCH DIRECTORATE

AIR FORCE CAMBRIDGE RESEARCH LABORATORIES

OFFICE OF AEROSPACE RESEARCH

UNITED STATES AIR FORCE

BEDFORD, MASSACHUSETTS

ACKNOWLEDGEMENT

TABLE OF CONTENTS

ABSTRACT

A shielded twin inner conductor transmission line is investigated as the vehicle for obtaining extremely road bandwidth nonreciprocal coaxial components. The inner conductors are coupled through a coextensive magnetized ferrite rod and a process completely analogous to Faraday rotation transfers energy between the conductors. As is typical of Faraday rotation the rotational process is essentially flat for frequencies of twice the magnetization and higher. The TEM transmission structure offers no dispersion but does limit the highest frequencies both through higher mode processes and through the limitations of the bandwidth of the transitions at the terminals to standard coaxial line. The principles of gyromagnetic coupling are discussed and analyzed and a formulation is determined which covers the simultaneous effects of reciprocal and nonreciprocal coupling. Means are discussed to eliminate reciprocal coupling as well as backward wave coupling, both of which add undesirable effects to the Faraday rotation phenomenon. Experimental results confirm the large bandwidth produced with nonreciprocal coupling where, typically, flat coupling was observed between 1.8 and 5.6 kmc. Discussions are given on the constructional difficulties in realizing an experimental broadband circulator, but the nonreciprocal properties are demonstrated in a narrow band device.

I.   INTRODUCTION

This is the final report of a study by Merrimac Re-
search and Development Inc. on the development of extreme-
ly broadband ferrite devices. These devices are intended
to include circulators, isolators, gyrators, baluns, and
flat variable couplers. This class of devices is based on
a novel generic structure for which Merrimac has recently
been awarded a patent. The study reported here was a theo-
retical and experimental investigation of the feasibility,
limitations and potentialities of this class of devices.

The first conception of these devices visualized a fer-
rite rod symmetrically disposed between an inner conductor
pair which in turn is sheathed by an outer conductor, as
shown in Figure 1. The modes of the system were conceived
to be those in which the two inner conductors bore a quad-
rature relationship in either leading or lagging phase. An-
alysis indicated that a phenomenon akin to Faraday rotation
would occur in which power flow would be nonreciprocally ro-
tated from one of the wire pairs to the other, leading to
the possibility of nonreciprocal interaction between the
terminals connected to the various ends of the wire pair.
Since the interaction with the ferrite is closely identi-

fied with the physics of the interaction effects in an un-
bounded medium, which leads to an essentially constant ro-
tation rate, it was felt that the combination of Faraday
rotation with a nondispersive TEM system would lead to the
realization of the broadest band microwave nonreciprocal
components yet constructed.

While the first conceptions have proved correct, there
were nevertheless important omissions. It is the intent of
this, the final report, to establish some generalizations
over the preceeding reports and to dwell on some of the fol-
lowing considerations:

1. Was the initial intuitive recognition of the nor-
mal modes in the ferrite-loaded guide correct?

2. What are the modes of the system for arbitrary
cross-sections of the inner conductors and ferrite?

3. What are the modes of the system in the presence
of dielectric coupling, and how does it affect de-
vice performance?

4. How are the effects of backward wave coupling to
be mitigated?

5. What are the considerations associated with a
greater multiplicity of inner conductors?

2

6. What are the considerations in determining an
   optimum structure?

In the course of the contract investigations the re-
sults of these considerations were taken into account in an
experimental program to verify the validity of this novel
approach to a class of extremely broadband ferrite devices.
This report also describes the manner in which the princi-
pal, and several auxiliary, experimental investigations were
conducted, and also presents the results of these measure-
ments. Additional comments in this regard are made later
in the Introduction.

We begin our theoretical considerations in the most
fundamental way by recognizing that the application of mag-
netic field to the gyromagnetic material produces a Zeeman
splitting of the initial degeneracy of the ground state en-
ergy level. It was Lorentz who recognized that Faraday ro-
tation was an interference phenomenon between the two new
states where the slight difference in refractive index be-
tween these states caused a continuous change in phase of
the admixture, producing a continuous rotation of a linear
polarization in an infinite medium.

Faraday rotation is constant with frequency up to some

3

limiting value imposed by the proximity of adjacent energy levels. The limiting frequency is generally much beyond the concern of the microwave designer since adjacent levels differ by energies comparable to exchange energy or higher, and are much beyond the reach of microwave frequencies.

The flatness of Faraday rotation requires that the signal frequency be large compared to the splitting of the energy states. The splitting is a cooperative relationship between the applied magnetic field and the internal field of the medium produced by the induced magnetization of the sample. The flatness stems from the fact that the susceptibility of the ferrite diminishes as $\frac{1}{\omega}$ far away from the spin resonance frequency which, in conjunction with the increasing electrical length of the system with frequency, provides a constant interaction.

We find thus that the medium tends to produce flat rotation but that there are constraints imposed on the transmission system in view of the above discussion.

1. The transmission system must be nondispersive.

2. The transmission system, in conjunction with the gyromagnetic material, possesses two initially degenerate states split by the application of

4

magnetic field.

3. The minimum frequency of operation must be large compared to that of gyromagnetic resonance.

We shall view Faraday rotation in a somewhat broader sense than that corresponding to a physical rotation. We shall consider, instead, a use of the gyromagnetic material to provide a constant interference between the products of the splitting of the degenerate modes, but which is not necessarily evidenced as an angle of a linear polarization. It is possible, therefore, to forego a system possessing rotational symmetry which supports degenerate linear polarizations and which makes the use of an angle meaningful, in favor of a more general system possessing other advantages.

Let us discuss first the disadvantages of a rotationally symmetric transmission system. It must, first of all, contain an outer circularly cylindrical conductor for shielding purposes. If it contained that alone, it would correspond to the conventional usage of a gyromagnetic element in a dispersive waveguide. The simplest TEM structure contains a single coaxial conductor and clearly provides but a single mode, in contrast to the necessary two. The next higher structure which makes the notion of angle meaningful

5

is that of three inner conductors arranged on a circle co-
axial with the outer conductor. This system, however, is
trimodal which leads to the possibility of complication due
to spurious interference by the redundant mode. A specific
example of such interference is the splitting effect of the
dielectric portion of the central ferrite rod. It splits
the zero phase sequence away from the degenerate doublet
which has a Zeeman splitting with the applied magnetic field.
Hence, the triple conductor coax, in the presence of a mag-
netic field, becomes a three nondegenerate mode system clear-
ly not directly applicable to Faraday rotation.

Added dielectric compensation which equalizes the ener-
gy storage in the zero sequence and circularly polarized
modes is indeed possible. It does, however, provide com-
plications in that, with the exception of the case of com-
plete uniform dielectric filling, the energy storage com-
pensation adds frequency sensitivity. Complete filling with
a dielectric constant typically of order 13 would effect the
compensation but is felt to increase loss significantly.

We thus break with a tradition of Faraday rotation and
seek its accomplishment without regard to rotational sym-
metry, but through the use of a shielded twin-conductor sys-

6

tem. While the notion of angle is not here readily apparent, we shall show in a later section that it still obtains in a geometrically meaningful fashion. With accessible terminals at each end of each of the conductors we have a four-port which is generally nonreciprocal because of the gyromagnetic medium. This fourport can be made to provide a variety of nonreciprocal components as a function only of the degree of nonreciprocal coupling and the nature of the terminal interconnections.

This report will deal with the analytical and experimental methods for the design of twin-conductor nonreciprocal fourports. It will focus on the more detailed considerations of design, the means of evaluation, and some actual experimental results. One of the major aspects of the design, the specific configuration of the twin-conductor cross-section leading to optimal interaction, has not been investigated completely in this report, and should be the subject of more extensive investigation. Nevertheless, feasibility has been established and the structure functions in much the manner anticipated. Numerical details will be given in the section on experimental results.

7

II. THEORY OF THE NONRECIPROCAL TWO-WIRE COUPLER

In its simplest view, the twin-conductor system is a forward wave two-wire coupler with reciprocal coupling occurring via the dielectric constant of the ferrite rod and nonreciprocal coupling taking place through the gyromagnetic portion. In the treatment to follow, the coupling will be assumed relatively light and a perturbation viewpoint will be presumed.

1. Gyromagnetic Coupling

Let us first consider the effect of gyromagnetic coupling. There exist two states which, to first order, are split symmetrically about the unperturbed state. The splitting is proportional to the magnetization and the resulting states are related to the direction of applied magnetic field. There can be no preferred direction of magnetic field because these states are identical with field reversal except that they are individually interchanged. Because of the lack of preference of field direction the magnitude of excitation of each of the conductors is the same in both states but we may anticipate that it is through phase relationships alone that the two states are distinguished. We now develop just these relationships by investigating the physical significance

8

of field reversal.

The direction of the mangetic field determines the direction of spin precession and, in a perfectly reactive medium, corresponds to a time reversal of the spin dynamics. Hence, a field reversed state leads to a time reversal or complex conjugacy of those field terms determined uniquely by the magnetic coupling.

Let Δ be the change in propagation constant in one of the new diagonalized modes in the presence of the magnetic field. Corresponding to this mode is a voltage distribution on the two conductors v_1 and v_2, respectively, which is a function only of the magnetic coupling and the geometry. The quantities v_1 and v_2, indeterminate in the unperturbed degenerate state, are uniquely related only through the applied magnetic field. With field reversal, which exchanges states, each state maps into its conjugate from the foregoing arguments.

We employ a column vector notation to describe the two states of the system, which are

$$\Psi_1 = \left\| \begin{matrix} v_1 \\ v_2 \end{matrix} \right\| \qquad \Psi_2 = \left\| \begin{matrix} v_1^* \\ v_2^* \end{matrix} \right\|$$

Corresponding to state 1 is the propagation constant β_1 and to state 2 the constant β_2. We have from previous considerations, that

9

$$\beta_1 = \beta_0 - \Delta$$
$$\beta_2 = \beta_0 + \Delta$$

where β_0 is the unperturbed propagation constant. The two states may then be placed in z dependent form to become

$$\Psi_1(z) = \binom{V_1}{V_2} e^{-i(\beta_0 - \Delta)z}$$

$$\Psi_2(z) = \binom{V_1^*}{V_2^*} e^{-i(\beta_0 + \Delta)z}$$

(1)

Equation (1) suffices to derive the transmission properties of the uniform system, and we shall investigate these properties shortly. As a preliminary to that consideration, however, we must be concerned with the means of exciting this system from accessible terminals without setting up backscattering processes which will complicate forthcoming developments.

Let us consider the two-wire coupled line of Figure 1 prior to the introduction of the gyromagnetic material. There is little loss in the generality of the conclusions we seek if we assume that the cross-section is symmetric about some axis for the considerations of scattering at the terminals. Assume generator impedances of unity and symmetric and antisymmetric characteristic impedances of the two-wire structure of Z_S and Z_A, respectively.

It is apparent from first principles that coupling generally occurs between ports 1 and 2. Let us assume for

10

FERRITE

Hdc
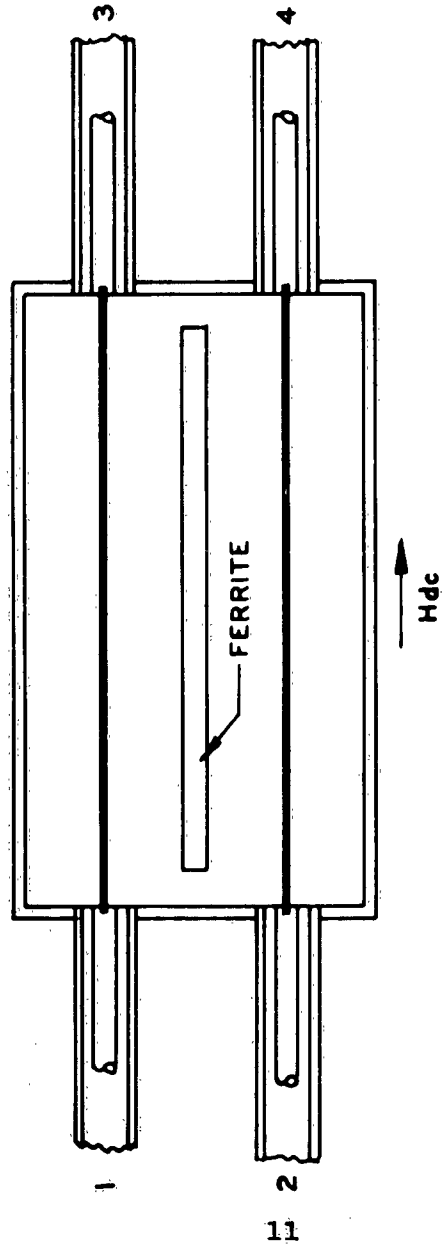
FIGURE 1—TWO WIRE COUPLED LINE

the moment that ports 3 and 4 were infinitely distant and that all energy incident upon them were absorbed in transmission line losses. Then the characteristic impedances Z_S and Z_A represent actual input impedances with symmetric and antisymmetric excitations at ports 1 and 2. Figure 2 shows the equivalent network existing between ports 1 and 2 which characterizes these impedances for the appropriate excitations. It is clear that only for $Z_S = Z_A$ is there an infinite directivity between ports 1 and 2. Two directly determinable features result from Figure 2:

a) The network image impedance is given by the geo-
metric mean of Z_S and Z_A.

b) The network insertion loss operating between image
terminations is given by

$$L_{db} = 20 \log \left[\frac{\sqrt{Z_S} + \sqrt{Z_A}}{\sqrt{Z_S} - \sqrt{Z_A}} \right]$$

The insertion loss expression demonstrates that a 20% difference between Z_S and Z_A leads to roughly a 26db coupling between ports 1 and 2. Figure 3 shows the variation of coupling over a range of Z_S/Z_A.

Corresponding to the symmetric mode on a two-wire line of length ϕ , there is a transfer function between unit

12
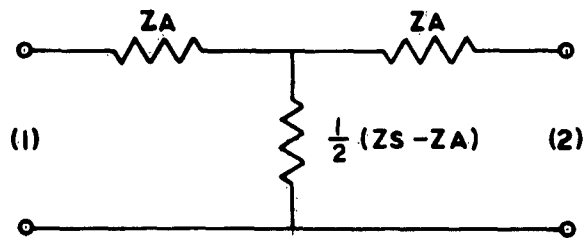
FIGURE 2-TWO PORT EQUIVALENT FOR
INFINITE LENGTH COUPLER
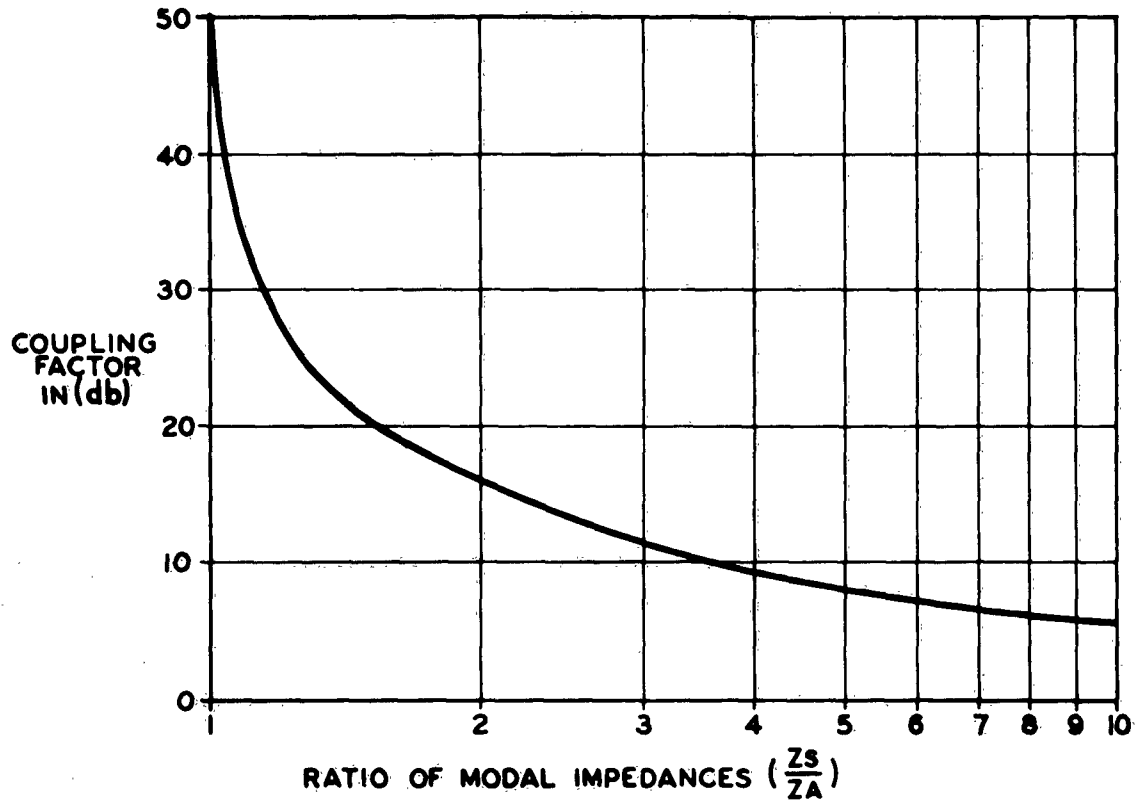
FIGURE 3—RESIDUAL BACKWARD COUPLING VERSUS
MODAL IMPEDANCE RATIO FOR INFINITE
LENGTH COUPLER

13

impedance terminations, having the form

$$\frac{1}{\cos\phi + \frac{1}{2}\,(Z_S + 1/Z_S)\,\sin\phi}$$

and a reflection coefficient of the form

$$\frac{i\,(Z_S - 1/Z_S)\,\sin\phi}{\cos\phi + \frac{1}{2}\,(Z_S + 1/Z_S)\,\sin\phi}$$

Identical relations pertain to the antisymmetric mode. A combination of these quantities provides the following scattering parameters:

$$S_{11} = \frac{i}{2}\,\sin\phi\left[\frac{Z_S - 1/Z_S}{\cos\phi + \frac{1}{2}\,(Z_S + 1/Z_S)\,\sin\phi} + \frac{Z_A - 1/Z_A}{\cos\phi + \frac{1}{2}\,(Z_A + 1/Z_A)\,\sin\phi}\right]$$

$$S_{12} = \frac{i}{2}\,\sin\phi\left[\frac{Z_S - 1/Z_S}{\cos\phi + \frac{1}{2}\,(Z_S + 1/Z_S)\,\sin\phi} - \frac{Z_A - 1/Z_A}{\cos\phi + \frac{1}{2}\,(Z_A + 1/Z_A)\,\sin\phi}\right]$$

$$S_{13} = \frac{1}{2}\left[\frac{1}{\cos\phi + \frac{1}{2}\,(Z_S + 1/Z_S)\,\sin\phi} + \frac{1}{\cos\phi + \frac{1}{2}\,(Z_A + 1/Z_A)\,\sin\phi}\right]$$

$$S_{14} = \frac{1}{2}\left[\frac{1}{\cos\phi + \frac{1}{2}\,(Z_S + 1/Z_S)\,\sin\phi} - \frac{1}{\cos\phi + \frac{1}{2}\,(Z_A + 1/Z_A)\,\sin\phi}\right]$$

14

When the conductors of the wire pair couple significantly to one another, there is a sensible difference in mode distributions corresponding to the electric and magnetic walls at the symmetry plane. The antisymmetric impedance Z_A is always less then Z_S since the electric wall defines a lower impedance than does the magnetic, and the equations above demonstrate considerable scattering within the fourport structure even prior to the insertion of the ferrite.

These equations show, however, that such scattering disappears in the limit as $Z_S \longrightarrow Z_A \longrightarrow 1$, in which case only S_{13} remains finite, causing the scattered coupling to disappear. This same limiting condition, however, is one in which the center conductors are made extremely small and close to the outer conductor, with only infinitesimal energy left at the plane of symmetry where one might have hoped for strong field interactions with the ferrite medium.

It appears then that the terminal accessibility conditions and the gyromagnetic coupling are not simultaneously compatible. The situation is resolved, however, by introducing the terminals into the transmission system in

15

regions where the central conductors are infinitesimally coupled, and by then gradually tapering the conductors into regions of strong coupling.

In the analysis to follow we shall now be capable of defining power flow at a port unambiguously. If the gyromagnetic coupling is broken as the internal conductor goes from a uniform to a tapered region, then the power flow on that conductor is preserved and measured at the output and the emergent wave amplitude at that port will differ by only a scale factor from that on the conductor prior to entering the taper region. In the ensuing development, all references to calculation of power will implicitly assume measurement in just this fashion. In this context it is important to note that the "voltages" defined in the state functions of the system are not the values they actually take on, but are those values referred to the output ports.

We shall now seek to determine the network properties of the fourport in the presence of gyromagnetic coupling only. The symmetric and antisymmetric modes are no longer adequate states of the system and we must then return to the representational form of equation (1) for appropriate description. Let us consider a unit amplitude

16

incident at port 1 in Figure 1 with a zero incidence at port 2. Let the excitation of the system be characterized as

$$A \Psi_1(z) + B \Psi_2(z)$$

From the boundary conditions at $z = 0$ we have

$$A v_1 + B v_1^* = 1$$

and

$$A v_2 + B v_2^* = 0$$

with the result that

$$A = \frac{v_2^*}{v_1 v_2^* - v_2 v_1^*}$$

and

$$B = \frac{-v_2}{v_1 v_2^* - v_2 v_1^*}$$

Let $V_1(z)$ be the voltage amplitude measured on conductor 1 as a function of z, and correspondingly for $V_2(z)$. In terms of the values of A and B we determine that

$$V_1(z) = \frac{e^{-i\beta_0 z}}{v_1 v_2^* - v_2 v_1^*} \left[v_1 v_2^* e^{i\Delta z} - v_2 v_1^* e^{-i\Delta z} \right] \qquad (2a)$$

and

$$V_2(z) = \frac{i z e^{-i\beta_0 z}}{v_1 v_2^* - v_2 v_1^*} \sin \Delta z \qquad (2b)$$

17

If g_1 and g_2 are the output port conductances associated with conductors 1 and 2, then conservation of power required that

$$\left| V_1(z) \right|^2 g_1 + \left| V_2(z) \right|^2 g_2 = \text{constant}$$

Since (2b) is a sine function, (2a) must be a cosine so that

$$v_1 v_2^* = -v_2 v_1^* \qquad ,$$

producing a quadrature phase between v_1 and v_2. Again, from power conservation, we demand that

$$\left| v_1 v_2 \right|^2 g_1 = \left| v_2 \right|^4 g_2$$

so that

$$\left| v_2 \right|^2 = \frac{g_1}{g_2} \left| v_1 \right|^2 \qquad\qquad (3)$$

We may, with no loss in generality, choose $v_1 = 1$ and $v_2 = i \left(\frac{g_1}{g_2} \right)^{\frac{1}{2}}$ with the result that equations (2a) and (2b) become

$$V_1(z) = e^{-i\beta_0 z} \cos \Delta z \qquad\qquad (4a)$$

$$V_2(z) = e^{-i\beta_0 z} \left(\frac{g_1}{g_2} \right)^{\frac{1}{2}} \sin \Delta z \qquad\qquad (4b)$$

18

If we define $\Theta = (\Delta\beta)L$, where $\Delta\beta$ is the difference between the propagation constants of the two magnetically split states and L the length of the interaction region, then, since $\Delta\beta = 2\Delta$, we have, to within the unperturbed phase constant in β_0,

$$V_1(L) = \cos\frac{\Theta}{2} \qquad\qquad (5a)$$

$$V_2(L) = -\left(\frac{g_1}{g_2}\right)^{\frac{1}{2}}\sin\frac{\Theta}{2} \qquad\qquad (5b)$$

The term $V_1(L)$ is the scattering term S_{31} where the port notation is defined through Figure 1. If an applied voltage of $g_1^{-\frac{1}{2}}$ were applied at port 1 then the resulting voltage at port 4 is $g_2^{-\frac{1}{2}}$ producing, from (5b), a value $S_{41} = -\sin\frac{\Theta}{2}$. Repeating similar arguments applied to port 2 produces scattering coefficients $S_{42} = \cos\frac{\Theta}{2}$ and $S_{32} = \sin\frac{\Theta}{2}$.

From Figure 4, it is observed that the scattering from ports 3 and 4 are obtained by symmetry from 1 and 2 by rotating the guide end for end, mapping 3 into 2, mapping 4 into 1, reversing the field with a consequent sign change on Θ, and interchanging g_1 and g_2. We thus find $S_{24} = \cos\frac{\Theta}{2}$, $S_{14} = \sin\frac{\Theta}{2}$, $S_{13} = \cos\frac{\Theta}{2}$, and $S_{23} = -\sin\frac{\Theta}{2}$.

19
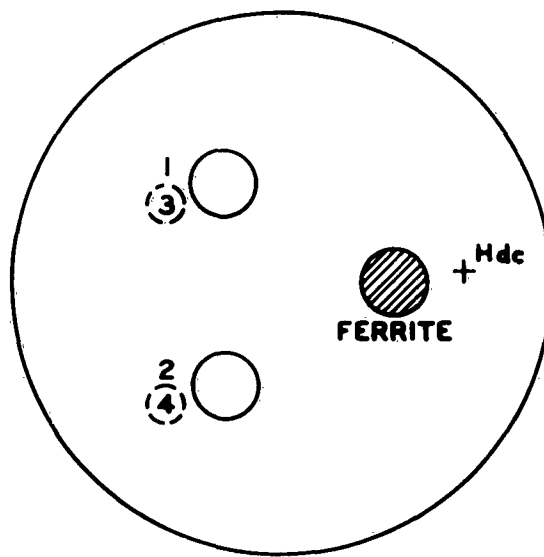
FIGURE 4—TRANSVERSE CROSS-SECTION OF FERRITE LOADED LINE

The scattering matrix is, therefore,

$$S = \begin{Vmatrix} 0 & 0 & \cos\frac{\theta}{2} & \sin\frac{\theta}{2} \\ 0 & 0 & -\sin\frac{\theta}{2} & \cos\frac{\theta}{2} \\ \cos\frac{\theta}{2} & \sin\frac{\theta}{2} & 0 & 0 \\ -\sin\frac{\theta}{2} & \cos\frac{\theta}{2} & 0 & 0 \end{Vmatrix} \tag{6}$$

Equation (6) is the scattering matrix for the ideal fourport which follows from pure gyromagnetic coupling. It is a nonreciprocal rotator identical in form, with appropriate identification, to that of the Faraday rotator in a rotationally symmetric system. Once this recognition is made circulators, isolators, gyrators, etc., are readily constructed. We shall now show such constructions.

(a) Circulators

Connect ports 3 and 4 to a coaxial hybrid as shown in Figure 5. Let $3'$ be a symmetry port of the hybrid and $4'$ an antisymmetry port. We then have

$$b_3 = \frac{1}{\sqrt{2}} (b_3' + b_4')$$

$$b_4 = \frac{1}{\sqrt{2}} (b_3' - b_4')$$

where the b and b' terms are the emergent wave vector terms corresponding to the unprimed and primed ports, with corresponding relationships for the incident waves. We obtain

21
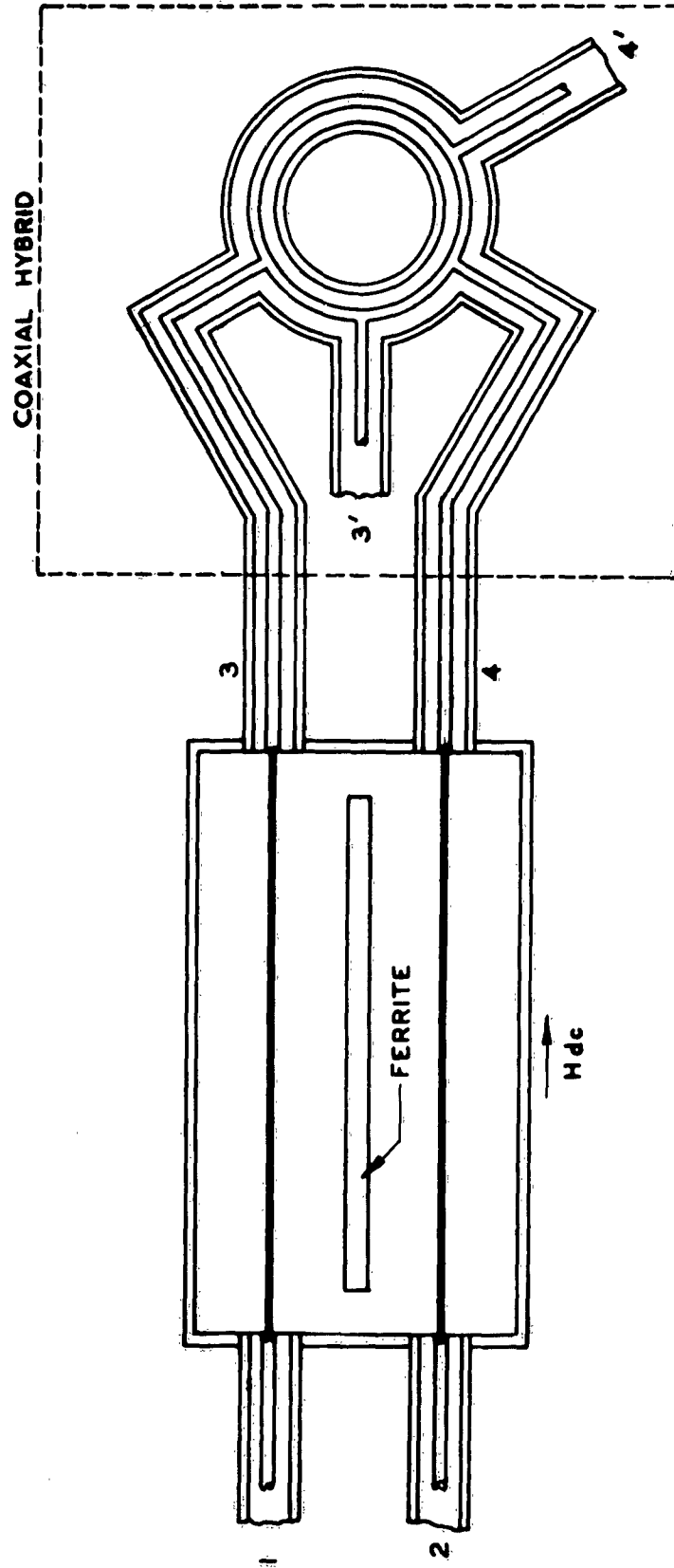
FIGURE 5—FOUR PORT CIRCULATOR

the new scattering matrix transformed to ports 3' and 4'.

$$S = \frac{1}{\sqrt{2}} \begin{Vmatrix} 0 & 0 & \cos\frac{\theta}{2}+\sin\frac{\theta}{2} & \cos\frac{\theta}{2}-\sin\frac{\theta}{2} \\ 0 & 0 & \cos\frac{\theta}{2}-\sin\frac{\theta}{2} & -\cos\frac{\theta}{2}-\sin\frac{\theta}{2} \\ \cos\frac{\theta}{2}-\sin\frac{\theta}{2} & \cos\frac{\theta}{2}+\sin\frac{\theta}{2} & 0 & 0 \\ \cos\frac{\theta}{2}+\sin\frac{\theta}{2} & -\cos\frac{\theta}{2}+\sin\frac{\theta}{2} & 0 & 0 \end{Vmatrix} \quad (7)$$

Choosing $\theta = \frac{\pi}{2}$, equation (7) becomes

$$S = \begin{Vmatrix} 0 & 0 & 1 & 0 \\ 0 & 0 & 0 & -1 \\ 0 & 1 & 0 & 0 \\ 1 & 0 & 0 & 0 \end{Vmatrix} \quad (8)$$

Equation (8) is that of an ideal fourport circulator. Since this circulator requires a hybrid, frequency sensitivity is implicit in the use of the antisymmetric arm. A simple shunt tee, with properly matched impedances, substituting for the hybrid, equivalently reflects the non-existent antisymmetric port and transforms the fourport to the relatively frequency insensitive threeport shown in Figure 6.

23
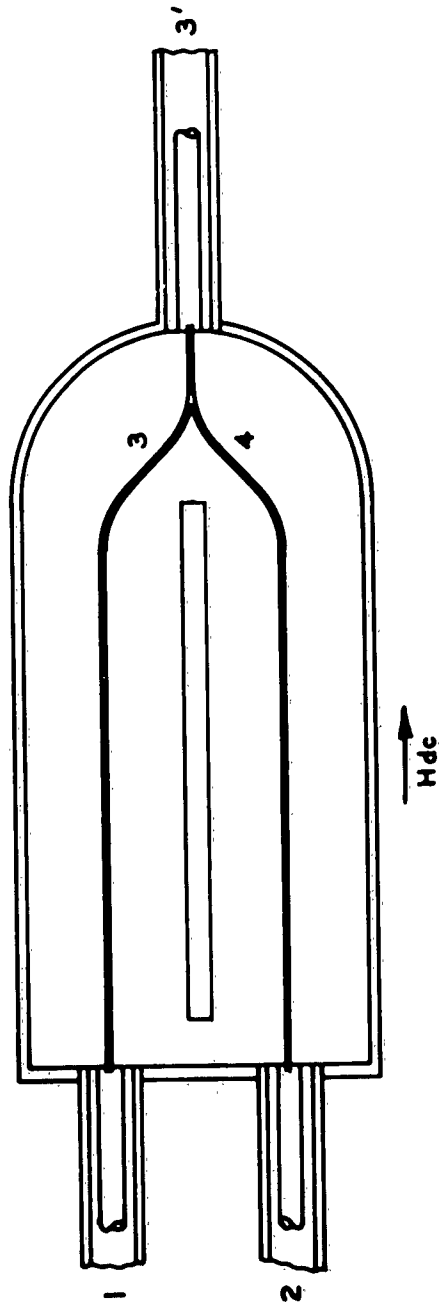
FIGURE 6—THREE PORT CIRCULATOR

24

(b) <u>Isolator</u>

The isolator is formed by loading one port of the threeport circulator. We derive this directly from (8) by shorting port 4' and placing a matched load on port 2. This leads directly to the relationship

$$
\left\| \begin{matrix} b_1 \\ b_3 \end{matrix} \right\|' = \left\| \begin{matrix} 0 & 1 \\ 0 & 0 \end{matrix} \right\| \left\| \begin{matrix} a_1 \\ a_3 \end{matrix} \right\| \qquad (9)
$$

which demonstrates the validity of the procedure.

(c) <u>Gyrator</u>

A choice of $\Theta = \pi$ in (6) produces the scattering matrix

$$
S = \left\| \begin{matrix} 0 & 0 & 0 & 1 \\ 0 & 0 & -1 & 0 \\ 0 & 1 & 0 & 0 \\ -1 & 0 & 0 & 0 \end{matrix} \right\| \qquad (10)
$$

Equation (10) characterizes a degenerate fourport showing two uncoupled gyrators; one between ports 1 and 4, and the other between ports 2 and 3.

(d) <u>Balun</u>

Let a unit excitation be applied to terminal 1 of Figure 1. The scattering by the fourport is given by (6), producing the emergent vector

25

$$\begin{Vmatrix} 0 \\ 0 \\ \cos \frac{\Theta}{2} \\ -\sin \frac{\Theta}{2} \end{Vmatrix}$$

A choice of Θ of $\frac{\pi}{2}$ shows antiphase scattering to terminals 3 and 4. If conversely, the output excitation were fed back as an input, the new resulting output would be

$$\begin{Vmatrix} \cos \Theta \\ -\sin \Theta \\ 0 \\ 0 \end{Vmatrix}$$

The new output emerges at port 2, for $\Theta = \frac{\pi}{2}$, and not port 1. The fourport structure therefore provides a combination of unbalanced to balance transition with an isolator, if port 2 is terminated.

If an odd excitation is applied to terminals 1 and 2 respectively, producing an incident column vector,

$$\frac{1}{\sqrt{2}} \begin{Vmatrix} 1 \\ -1 \\ 0 \\ 0 \end{Vmatrix}$$

The emergent wave becomes

26

$$\frac{1}{\sqrt{2}} \left\| \begin{matrix} 0 \\ 0 \\ \cos\frac{\theta}{2} - \sin\frac{\theta}{2} \\ \cos\frac{\theta}{2} + \sin\frac{\theta}{2} \end{matrix} \right\|$$

For $\theta = \frac{\pi}{2}$, all the energy appears entirely at port 4. The isolator action is implicit in that incident energy at 4 produces an output at 1 and 2 respectively, of an even mode.

It has thus been demonstrated that a balun isolator may be constructed choosing either the balanced or the unbalanced mode as an input.

(e) Variable Directional Coupler

The variable coupler derives directly from (6) by varying θ as a function of magnetization. For all its non-reciprocity, equation (6) may be regarded as a directional coupler with a coupling related to nonreciprocal angle. Caution must be expressed in operating along the ferrite saturation curve because of initial disorder losses. However, recent ferrite developments have made initial losses minimal in the low field region, making this a practical mode of operation.

We have thus demonstrated that a two-wire system

27

suffices to construct all nonreciprocal components without redundancy and, in principle, with minimum dispersion. We shall, in the following section, continue to idealize the structure in terms of the losses of the medium, but we will consider the effects of adding reciprocal dielectric coupling to that of gyromagnetic coupling.

2. Combined Dielectric and Gyromagnetic Coupling

It has been demonstrated in the various preceding equations that the essential results are independent of the individual output port impedances.

For reasons to be made clear in later discussions which relate to minimizing magnetic losses, it is desirable to maintain the cross-section symmetric about a transverse axis. We shall so restrict our considerations from this point onward. Further, the voltage amplitudes will be taken to signify normalized wave amplitudes whose power is given by the squared magnitude.

Prior to formulating the two-wire coupling problem for the more general medium let us return to equation (1) relating to gyromagnetic coupling, choosing $v_1 = 1$ and $v_2 = i$, consistent with (3). We have

$$V_1(3) = Ae^{-i(\beta_0 - \Delta)3} + Be^{-i(\beta_0 + \Delta)3}$$

28

$$V_2(z) = Ae^{-i(\beta_0 - \Delta)z} - Be^{-i(\beta_0 + \Delta)z}$$

Differentiating both equations with respect to z we obtain

$$\frac{\delta V_1}{\delta z} = i\beta_0 V_1 + \Delta V_2$$

$$\frac{\delta V_2}{\delta z} = -\Delta V_1 - i\beta_0 V_2$$

which show that gyromagnetic coupling induces a form of description akin to that of a coupled line. It will be noted that the cross-coupling terms are real and that non-reciprocity is apparent in the difference of the signs of the coupling terms.

Reciprocal coupling, on the other hand, produces the coupled relationship

$$\frac{\delta V_1}{\delta z} = -i\beta_0 V_1 + i\gamma V_2$$

$$\frac{\delta V_2}{\delta z} = i\gamma V_1 - i\beta_0 V_2$$

Since, in a perturbation theory, the coupling terms are additive, the couplings due to both reciprocal and non-reciprocal effects are expressed by the following coupled equations:

$$\frac{\delta V_1}{\delta z} = -i\beta_0 V_1 + (i\gamma + \Delta)V_2 \tag{11a}$$

$$\frac{\delta V_2}{\delta z} = (i\gamma - \Delta)V_1 - i\beta_0 V_2 \tag{11b}$$

29

where γ represents the reciprocal forward wave coupling due to the dielectric constant of the ferrite rod.

The solution of equations (11) leads to the two propagation constants

$$\beta \pm = \beta_0 \pm \sqrt{\gamma^2 + \Delta^2} \tag{12}$$

and the relationship

$$V_2 \pm = \frac{\mp \sqrt{\gamma^2 + \Delta^2} \; V_1 \pm}{\gamma - i\Delta} = \frac{-}{+} e^{i\varphi} V_1 \pm \tag{13}$$

where $\emptyset$ = arctangent $\frac{\Delta}{\gamma}$.

The two modes are thus

$$\Psi_1(\mathfrak{z}) = \left\| \begin{matrix} 1 \\ e^{i\varphi} \end{matrix} \right\| e^{-i\left(\beta_0 - \sqrt{\gamma^2 + \Delta^2}\right)\mathfrak{z}} \tag{14a}$$

$$\Psi_2(\mathfrak{z}) = \left\| \begin{matrix} 1 \\ e^{i\varphi} \end{matrix} \right\| e^{-i\left(\beta_0 + \sqrt{\gamma^2 + \Delta^2}\right)\mathfrak{z}} \tag{14b}$$

Since $\theta = (\Delta\beta)L$, we observe that $\sqrt{\gamma^2 + \Delta^2} \; L = \frac{\theta}{2}$ and that (14a) and (14b) combine, through a procedure similar to that

30

$$S = \begin{Vmatrix} 0 & 0 & \cos\frac{\theta}{2} & ie^{-i\phi}\sin\frac{\theta}{2} \\ 0 & 0 & ie^{+i\phi}\sin\frac{\theta}{2} & \cos\frac{\theta}{2} \\ \cos\frac{\theta}{2} & ie^{-i\phi}\sin\frac{\theta}{2} & 0 & 0 \\ ie^{+i\phi}\sin\frac{\theta}{2} & \cos\frac{\theta}{2} & 0 & 0 \end{Vmatrix} \quad (15)$$

The reciprocal coupling evidently degrades the desired properties of the nonreciprocal fourport as may be observed by comparing (15) with (6), for values of ϕ other than $\frac{\pi}{2}$. It is instructive to repeat the analysis of the circulator as a major example to determine some measure of the degree of deterioration. We again seek the transformation of the scattering matrix relative to the new ports $3'$ and $4'$, and equation (15) becomes

$$S = \frac{1}{\sqrt{2}} \begin{Vmatrix} 0 & 0 & \cos\frac{\theta}{2}+ie^{-i\phi}\sin\frac{\theta}{2} & \cos\frac{\theta}{2}-ie^{-i\phi}\sin\frac{\theta}{2} \\ 0 & 0 & \cos\frac{\theta}{2}+ie^{i\phi}\sin\frac{\theta}{2} & -\cos\frac{\theta}{2}+ie^{-i\phi}\sin\frac{\theta}{2} \\ \cos\frac{\theta}{2}+ie^{i\phi}\sin\frac{\theta}{2} & \cos\frac{\theta}{2}+ie^{-i\phi}\sin\frac{\theta}{2} & 0 & 0 \\ \cos\frac{\theta}{2}-ie^{i\phi}\sin\frac{\theta}{2} & -\cos\frac{\theta}{2}+ie^{-i\phi}\sin\frac{\theta}{2} & 0 & 0 \end{Vmatrix} \quad (16)$$

31

A choice of $\Theta = \frac{\pi}{2}$ produces the fourport circulator scattering matrix given as

$$S = \begin{Vmatrix} 0 & 0 & e^{-i\frac{\delta}{2}}\cos\frac{\delta}{2} & ie^{-i\frac{\delta}{2}}\sin\frac{\delta}{2} \\ 0 & 0 & -ie^{i\frac{\delta}{2}}\sin\frac{\delta}{2} & -e^{i\frac{\delta}{2}}\cos\frac{\delta}{2} \\ -ie^{i\frac{\delta}{2}}\sin\frac{\delta}{2} & e^{-i\frac{\delta}{2}}\cos\frac{\delta}{2} & 0 & 0 \\ e^{i\frac{\delta}{2}}\cos\frac{\delta}{2} & -ie^{-i\frac{\delta}{2}}\sin\frac{\delta}{2} & 0 & 0 \end{Vmatrix} \tag{17}$$

where $\delta = \phi - \frac{\pi}{2}$, and is an index of reciprocal coupling.

Of particular interest is the threeport circulator because of its broadband properties. Short-circuiting the port at $4'$ transforms (17) into the three arm circulator scattering matrix:

$$S = \begin{Vmatrix} -\frac{i}{2}\sin\delta & -e^{-i\delta}\sin^2\frac{\delta}{2} & e^{-i\frac{\delta}{2}}\cos\frac{\delta}{2} \\ -\cos^2\frac{\delta}{2} & \frac{i}{2}e^{-i\delta}\sin\delta & -ie^{i\frac{\delta}{2}}\sin\frac{\delta}{2} \\ -ie^{i\frac{\delta}{2}}\sin\frac{\delta}{2} & e^{-i\frac{\delta}{2}}\cos\frac{\delta}{2} & 0 \end{Vmatrix} \tag{18}$$

The cross-coupled terms of (18) are unequally distributed. This arises from the fact that the fourport circulator permutation, according to (17), is 1, $4'$, 2, $3'$. Therefore, in the three arm circulator, the signal from 1 goes to 2 by twice the path of the transition $2-3'$, $3'-1$,

32

since 4' is shorted. Since port 3' is different in kind from 2, the terms in (18) bear no symmetric relationship.

The largest of the cross-coupled terms in (18) is that of S_{23}, which has a magnitude $\left|\sin\frac{\zeta}{2}\right|$. From (13) we observe that

$$\left|\sin\frac{\zeta}{2}\right| = \sin\frac{1}{2}\left|\text{arccot}\frac{\Delta}{\gamma}\right| \tag{19}$$

Assuming small reciprocal coupling we find the maximum value of the cross-coupling to be approximately $\frac{1}{2}\left|\frac{\gamma}{\Delta}\right|$. Hence, for a circulator directivity of 25db, the dielectric coupling must be below the gyromagnetic coupling by 19db.

These are several essential points which we may summarize in the construction of a two-wire "Faraday rotator" fourport:

1. Gyromagnetic coupling alone produces a scattering matrix corresponding to nonreciprocal rotation.

2. The added presence of dielectric reciprocal coupling degrades the rotation matrix.

3. The desired two-wire fourport characteristics are achieved only through the use of tapered transitions which "adiabatically" extract energy from each of the four accessible terminals of the two wire pair.

33

III SYMMETRIC TWO-WIRE LINES ELIMINATING DIELECTRIC COUPLING

The condition of dielectric degeneracy of the two modes of the two-wire system is achieved by equal relative energy density in the dielectric for each of them. With the application of magnetic field, it is only the gyromagnetic effect which splits the energy of the system, with the dielectric insensitive to any new admixture.

The simplest degenerate situation is shown in Figure 7. The ferrite is placed on the symmetry axis such that the relative dielectric energy storage is equal for the symmetry and antisymmetry modes. This equality is always afforded since the antisymmetry fields are stronger than the symmetry fields in the region close to the conductors, whereas, the reverse situation holds true at some distance away. The point locating the rod center is approximately at the point of E field equality between these two modes. It differs from an exact location there since the electric dipole energy must be integrated over the finite cross-section of the rod and the variation of the two field distribution functions differ quite significantly from each other.

By virtue of the tapered transformations, the characteristic impedances of the odd and even modes at the access-

ible terminals are identical so that equal generator power flows into each. The condition for equal electric energy storage normalized by modal power for degeneracy thus corresponds, in system usage, to the condition of actual E field equality. Hence the magnetic fields are also equal at the dielectric cross-over point, a precursor to the existence of circularly polarized fields at the ferrite.

According to (1) and (3) the voltage distributions on the wires are, for the symmetric case,

$$\psi_{1,2} = \left\| \begin{matrix} 1 \\ \pm i \end{matrix} \right\|$$

corresponding to the two magnetic states. This is so since we have assumed the electric degeneracy to exist and only the gyromagnetic coupling governs. While these modes properly diagonalize the system, it is convenient, nevertheless to consider them as admixtures. We have the identity

$$\left\| \begin{matrix} 1 \\ \pm i \end{matrix} \right\| = \frac{e^{\pm i \frac{\pi}{4}}}{\sqrt{2}} \left\| \begin{matrix} 1 \mp i \\ 1 \pm i \end{matrix} \right\| = \frac{e^{\pm i \frac{\pi}{4}}}{\sqrt{2}} \left[\left\| \begin{matrix} 1 \\ 1 \end{matrix} \right\| \mp i \left\| \begin{matrix} 1 \\ -1 \end{matrix} \right\| \right] \tag{20}$$

which shows the normal modes to be decomposable into odd and even modes with a quadrature phase relationship. We observe in Figure 7 that the symmetric and antisymmetric fields are perpendicular on the axis of symmetry. Since (20) indicates equal amplitudes of excitation of the symmetry antisymmetry modes, with a consequent equality of the electric and mag-

35
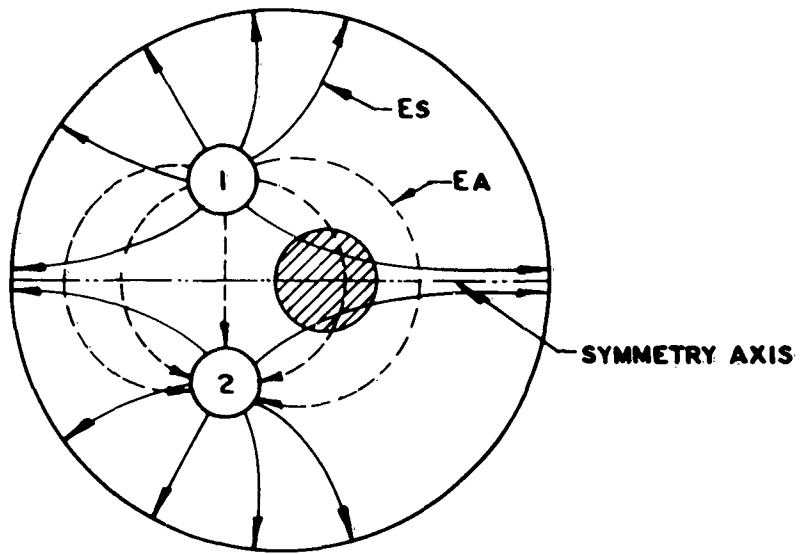
FIGURE 7-SYMMETRIC TWO-WIRE SYSTEM
CONTAINING FERRITE ROD

netic fields at the ferrite, the ferrite is located at a
point of circular polarization whose sense is dependent on
which of the normal modes is chosen to excite it.

It is now shown that this situation corresponds to
the least magnetic loss of all modes of operation. The non-
reciprocal electric angle θ defined in (5) is, as we shall
show, dependent on the square of the magnetic field. A pure
circular polarization produces a magnetic loss which is,
therefore, proportional to rotation. An elliptic polarization
is representable as having oppositely polarized components.
The magnetic loss in that case is related to the sum of the
powers corresponding to the two polarizations whereas the
rotation rate is proportional to the difference. Hence,
locating the ferrite at the dielectric cross-over point in
a symmetric cross-section corresponds to the most efficient
mode of operation because there then exists but one circular
sense.

The location of the ferrite at the point of cir-
cular polarization, while optimum, is by no means unique.
If the ferrite is placed at a point of unequal electric stor-
age, say at a point of excess symmetric field, then it is quite
possible to position a vernier dielectric member in a region

of stronger antisymmetric field in order to equalize energy storage. Aside from the greater magnetic loss of the system, as described earlier, there are two disadvantages inherent in the use of excess dielectric:

1. The perturbation treatment relating to a TEM transmission system becomes less valid.

2. The limiting frequency for which the static field distributions hold diminishes with added dielectric material, causing an earlier onset of frequency sensitivity.

Given the geometry of the wire pair transmission system the location of the ferrite for optimum performance is thus defined. It remains then to demonstrate the basis of the ferrite selection and to provide means for an estimation of its performance.

38

IV. <u>SELECTION OF FERRITE AND PROCEDURE FOR CALCULATING PERFORMANCE</u>

The susceptibility of a ferrite in a circular polarization basis is

$$\chi^{\pm} = \frac{1}{4\pi} \frac{\omega_m}{\omega_o \pm \omega} \tag{21}$$

where ω_m is the gyromagnetic frequency corresponding to the magnetization and is given by $4\pi M_s \gamma$, and ω_o is the precession frequency corresponding to the applied magnetic field.

Let $\underline{H}_o^{\pm}$ be the unperturbed circularly polarized rf magnetic fields, and let $\underline{H}_1^{\pm}$ be the corresponding fields inside the ferrite rod depolarized by the surface magnetic charge. If N is the transverse depolarizing factor, given by the isotropic value of 2π in the case of the rod, we have

$$\underline{H}_1 = \underline{H}_o - 2\pi \underline{M} = \underline{H}_o - 2\pi \chi \underline{H}_1$$

where $\underline{M}$ is the rf magnetization vector. From the above, we obtain

$$\underline{M} = \chi \underline{H}_1 = \chi (1 + 2\pi \chi)^{-1} \underline{H}_o$$

The perturbing energy which is proportional to the perturbation in propagation constant is

$$\underline{H}_o \cdot \underline{M}^* = \frac{|\underline{H}_o|^2 \chi}{1 + 2\pi \chi} \tag{22}$$

We find, in conjunction with (21), that

$$\Delta\beta_{\pm} \sim \omega \underline{H}_o^{\pm} \cdot \underline{M}^{\pm *} \sim \frac{|\underline{H}_o|^2 \omega_m \omega}{\frac{1}{2}\omega_m \pm \omega}$$

where it is assumed that the dc magnetic field just barely saturates the ferrite. Finally we observe from (23) that

$$\Delta\beta_+ - \Delta\beta_- = \frac{\mu_0 \omega_m |H_0|^2 A}{[1 - \frac{1}{4}(\frac{\omega_m}{\omega})^2] P} \qquad (24)$$

where (24) is now the actual relationship, where P is the integrated Poynting flux over the cross-section, and where A is the ferrite cross-section.

Equation (24) shows that a degree of dispersion is present in the Faraday rotation but is negligible for ω sufficiently large compared to ω_m. For ω greater than twice ω_m, the maximum deviation in rotation is about 6% occurring at the lowest end of the frequency band. Let us consider this deviation as applied to a fourport scattering matrix as represented by (7) in which θ takes on the value of 48° instead of 45°. We obtain

$$S = \begin{Vmatrix} 0 & 0 & .997 & -.053 \\ 0 & 0 & -.053 & -.997 \\ -.053 & .997 & 0 & 0 \\ .997 & .053 & 0 & 0 \end{Vmatrix}$$

which shows a cross-coupling in this worst case due to Faraday rotation dispersion equal to 25.5db below direct coup-
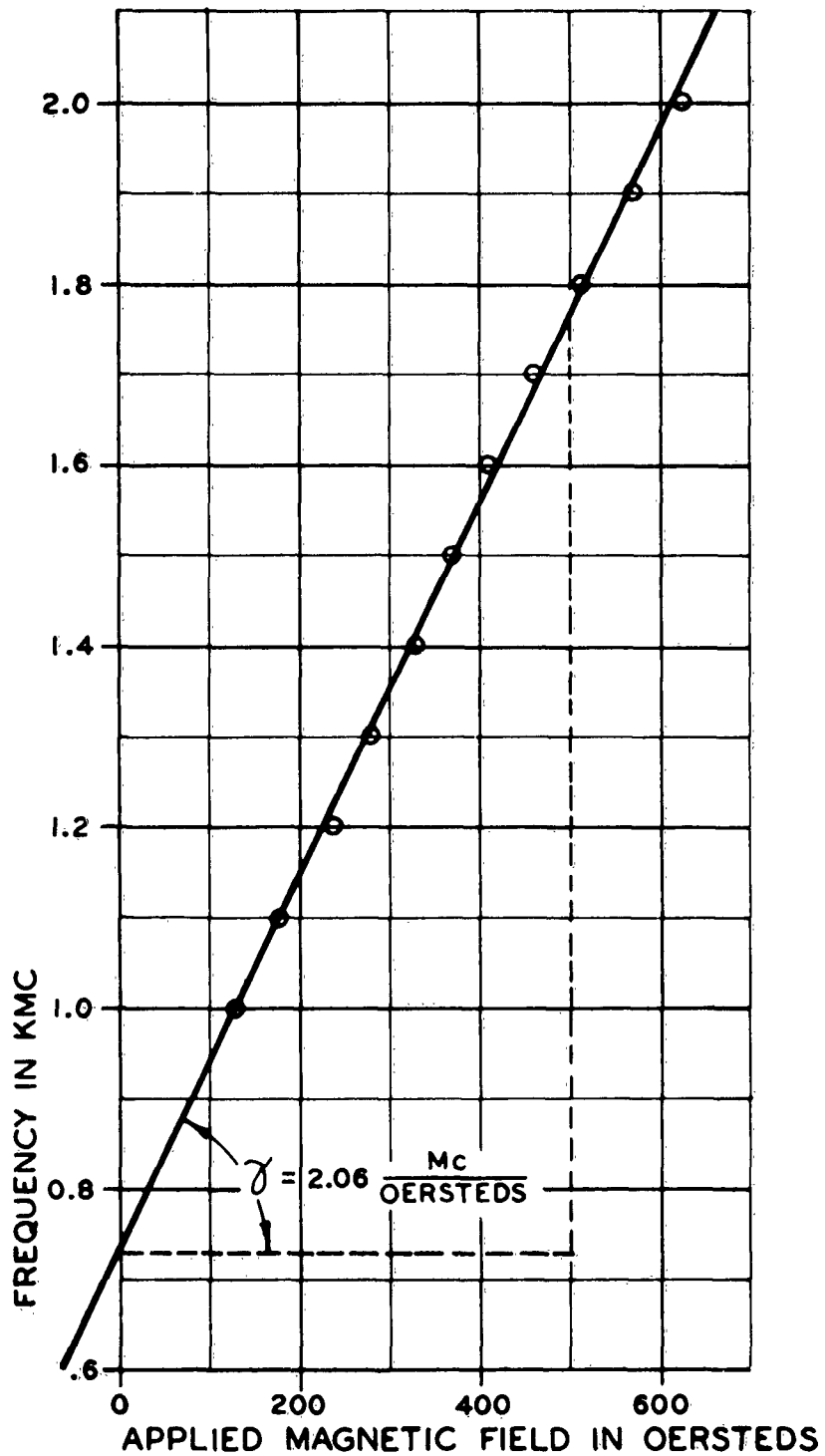
FIGURE 8 — EXPERIMENTAL DETERMINATION OF MAGNE—
TIZATION FREQUENCY AND GYROMAGNETIC
RATIO

41

ling. Since this number represents the maximum acceptable value from the point of view of design, we consider device operation to require that $\omega > 2\omega_m$.

The ferrite chosen for this project was an aluminum substituted yttrium iron garnet polycrystalline material designated as AN50 by the Kearfott Company, its manufacturer. The characteristics supplied by the manufacturer indicated a magnetization of 350 gauss and a gyromagnetic ratio γ of 2.1. These data were not, however corroborated by our experiments.

Figure 8 shows the experimental results for the resonance absorption frequency for this ferrite as a function of applied magnetic field. The resonance of the rod follows the Kittel formulation which follows in turn from the vanishing of the denominator of (22). The resonance frequency is given by

$$\omega = \omega_0 + \tfrac{1}{2}\,\omega_m$$

where $\omega_0 = \gamma H_{dc}$ and $\omega_m = 4\pi M_s \gamma$. The intercept on the ordinate provides the value $\tfrac{1}{2}\omega_m = 730$ mc and the slope shows a value of of $\gamma = 2.06$ mc/oe . Recapitulating, the measured data are

$\gamma = 2.06$ mc/oe, implying $g = 1.47$

$4\pi M_s = 720$ gauss

$\omega_m = 1460$ mc

42

These data in conjunction with (24) form the basis for estimating performance. Following the prescription given above for maximum acceptable Faraday rotation dispersion in terms of a 25db circulator directivity, the minimum operating frequency is 2.92kmc.

V.   ANALOG FIELD MEASUREMENTS

To examine the potentiality of the greatest variety of cross-sections for the realization of an acceptable non-reciprocal structure, it was deemed desirable to investigate them by a potential analog method as opposed to a calculational approach. The most convenient analog is formed using a constant surface resistivity sheet with equipotential surfaces painted on using low resistivity silver paint.

A four probe machine was constructed as shown in Figure 9. When one pair of probes reads a null, the other pair of probes are directed along an electric field line and their potential difference defines the electric field intensity. The measurements, while relative, are simply related to the actual field quantities through a knowledge of the scale factors and the sheet resistivity.

The structures actually studied are shown in Figure 10(a-c). In all cases there exists a symmetry axis bisecting the line of centers of the conductor pair, with a second symmetry axis at right angles to the first for Figures (a) and (b). In the analog measurements only a half or a quarter of the structure need be mapped and the symmetric and antisymmetric measurements correspond to an open or short circuit

LOCKING SCREW

CALIBRATED DIAL
AND 90° STOP

PIVOT POINT

SLIDING CARRIAGE

CALIBRATED DIAL
WITH 360° MOTION

STATIONARY BEAM

SCALE

PROBE PATTERN
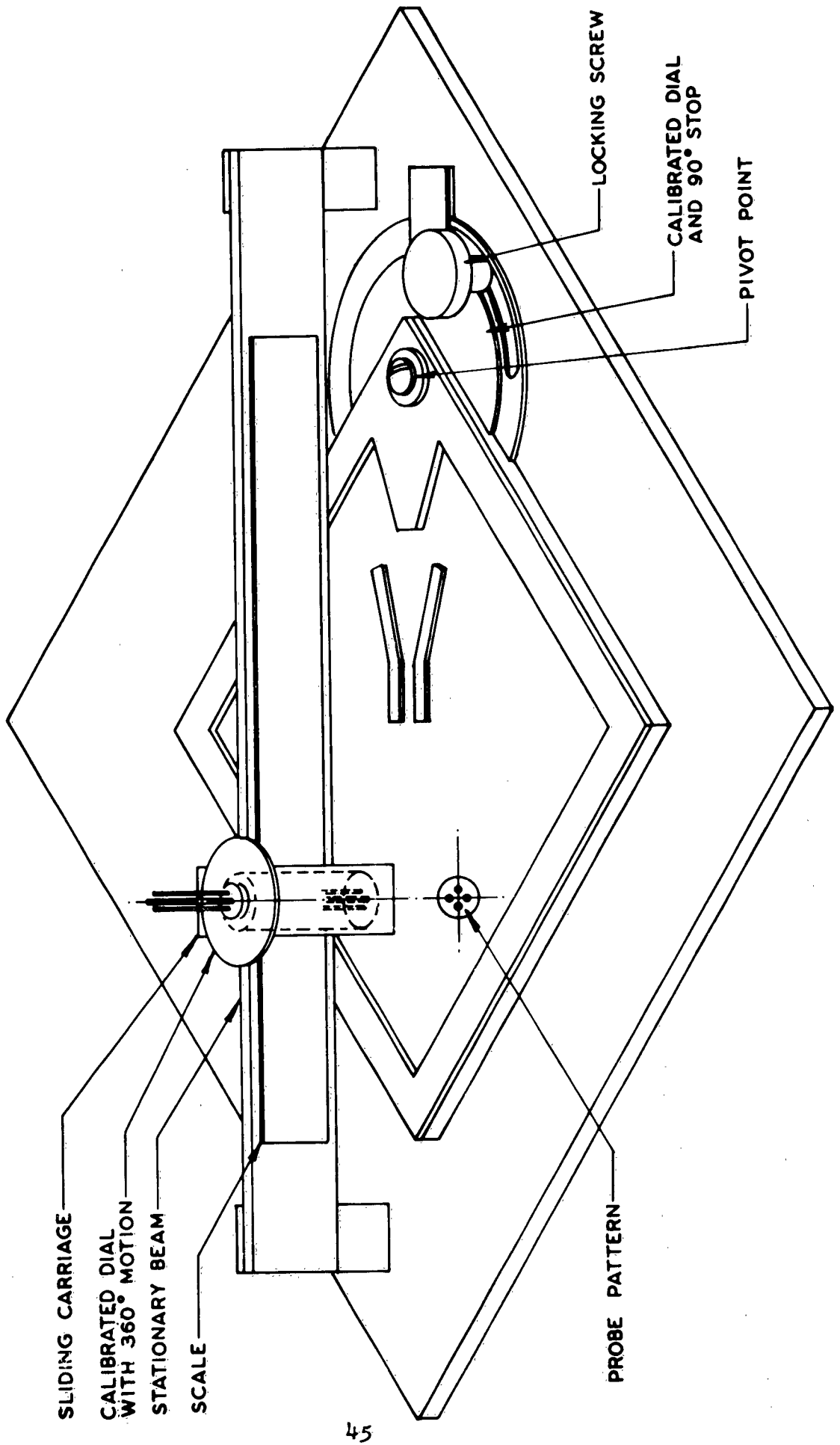
FIGURE 9 — ISOMETRIC VIEW OF FIELD PROBING DEVICE

45
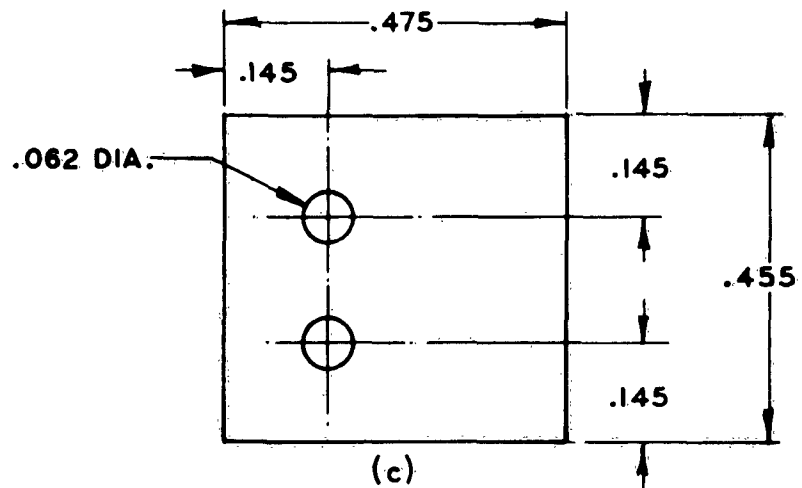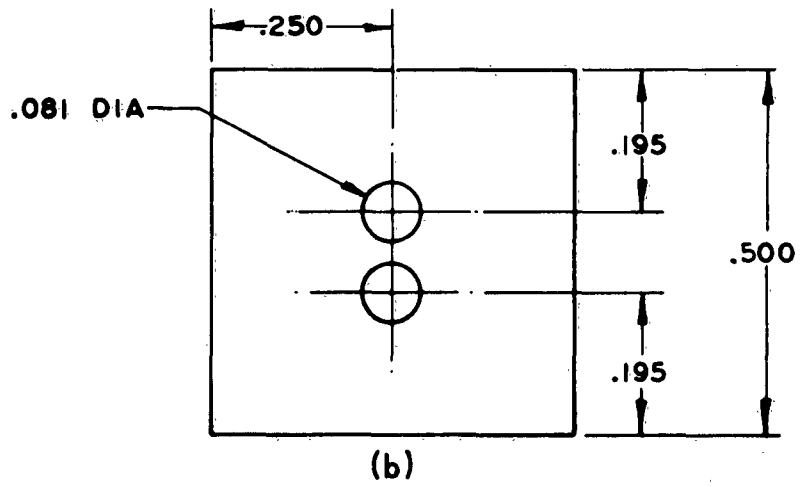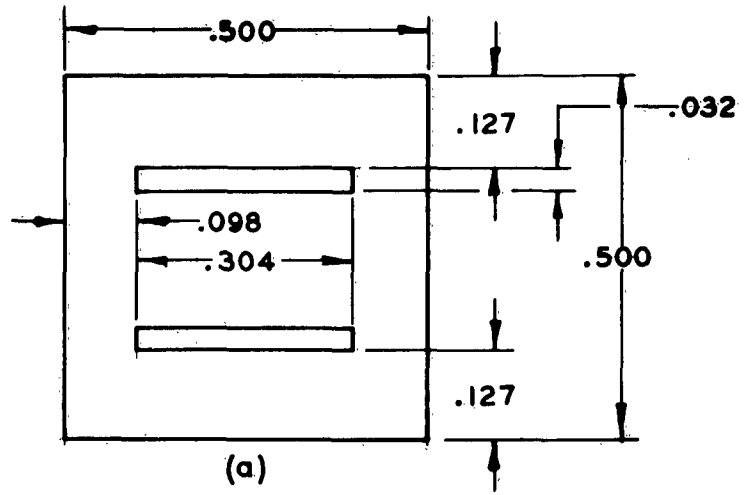
FIGURE 10-VARIOUS CROSS-SECTION TWIN CONDUCTOR LINES

along the first, if not only, symmetry axis. The second
symmetry axis, if it exists, is always a magnetic wall
for the TEM structure. Since the impedances differ, dif-
ferent voltages must be applied to the symmetric segment
of the structure to normalize it to unit power flow for
the odd and even modes, taking due account of the power
proportion flowing in the segment under investigation. The
purpose of this segmentation by symmetry is to obtain as
large a scaling factor as possible corresponding to the
limited surface of the resistance sheet having adequately
uniform properties. It has the further advantage of per-
mitting the use of standard resistance cards which are of
limited size.

The perturbation treatment of Faraday rotation in
nonreciprocally coupled lines indicates that the rotation
rate is proportional to the difference of the squared mag-
nitudes of the magnetic fields corresponding to the two
polarization senses, integrated over the cross-section of
the ferrite rod. The center of the rod is roughly at the
point of circular polarization but, as we shall show, the
polarization shifts rapidly from circular to linear in some
geometries, producing a small limiting rotation rate. This

is so, evidently, since the two circular polarization magnitudes tend towards equality, and only a small ferrite area exists for which this difference is marked.

It is instructive, in this regard, to view the results of Figure 11. This Figure shows the variation of odd and even electric fields along the first symmetry axis of the structure of Figure 10(a). Two features are immediately apparent, both operating to the detriment of this structure for the use intended:

(a) The circular polarization point is very close to the wall.

(b) There exists but a narrow region of substantial equality of the field amplitudes.

These features are, of course, not mutually exclusive and they tend to emphasize the limited region of usefulness of the ferrite rod.

It is unfortunate that the analog results were not available until relatively late in this study since they would have deemphasized the consideration of the structure of Figure 10(a) in favor of those of 10(b) and 10(c). Figures 10(b) and 10(c) follow from the intuitive consideration that circular rods will not "hoard" the odd mode as effectively
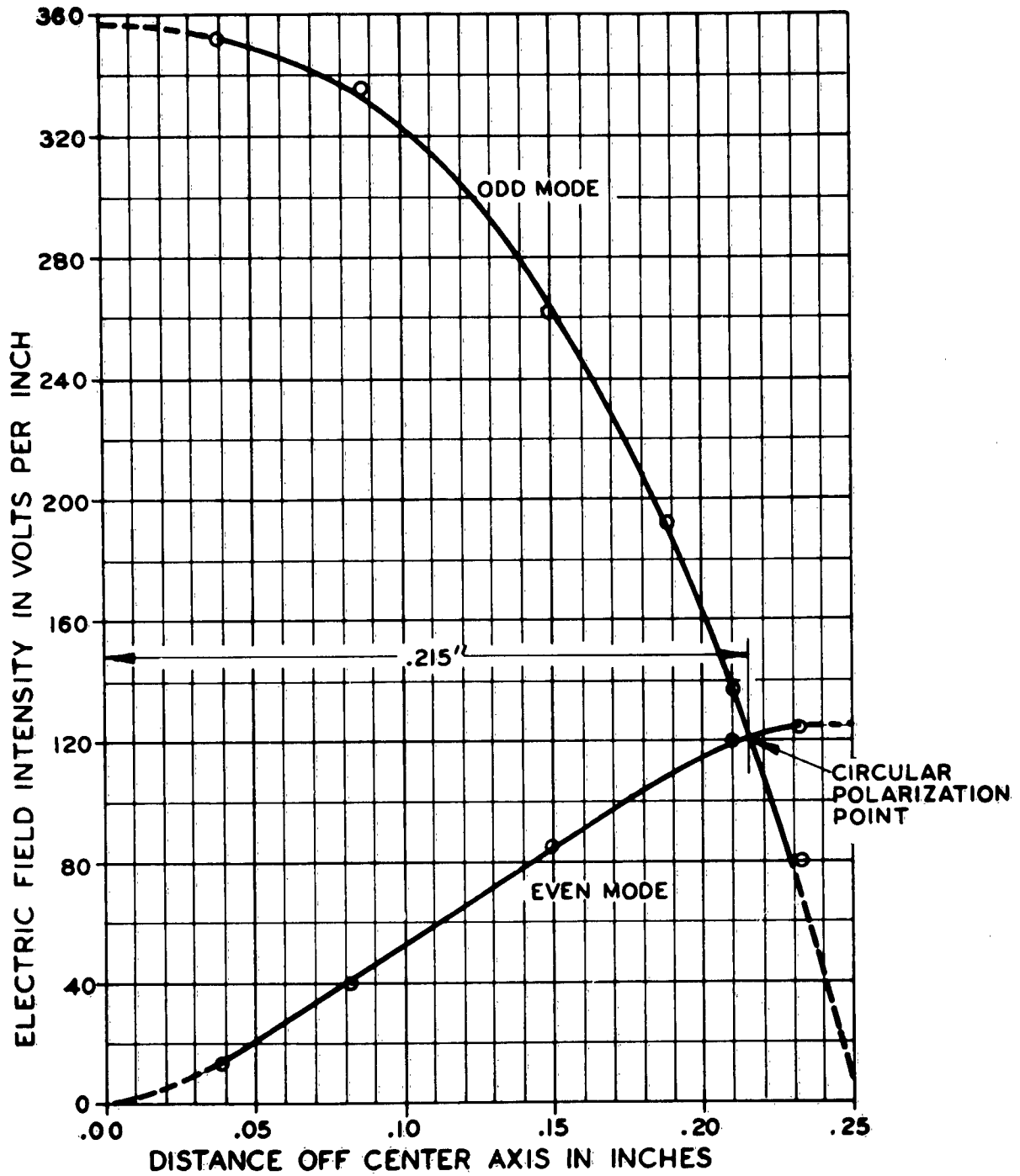
FIGURE II – ELECTRIC FIELD INTENSITIES IN THE MICRO-
WAVE STRUCTURE FOR EACH MODE VERSUS
POSITION OFF CENTER AXIS

49

as do the parallel strips nor would they as effectively suppress the even mode. Figure 10(b) possesses two possible advantages over 10(c):

(a) The wire pair is further from the walls, providing fairly strong field concentrations on both sides.

(b) It is possible to employ ferrite rods symmetrically on both sides with opposed axial magnetic fields, doubling the rotation rate.

The mitigating feature for 10(c), which actually makes it the more useful of the two, is that while the field concentration is weaker in the open region of the guide, it is more uniform than that of 10(b). If we choose not to employ the difficult magnetic field opposition implementation indicated above, we will find that 10(c) has in fact a superior rotation rate to 10(b).

The analog mapping can do no more than establish a rough index of performance of the ferrite loaded structure. Demagnetizing theory applies only to the situation of uniform incidence of the rf fields on an ellipsoidal body. Since the fields prior to the insertion of ferrite are so nonuniform, the best relative evaluation is that of inves-

50

tigating the initial distributions in the ferrite-free region, and roughly averaging the circular polarization content of the region to be occupied by the ferrite. We assume then that the ferrite demagnetization applies to this averaged value.

Two indicators seem important in evaluating general performance corresponding to a specific geometry:

(a) A measure of the area over which the initial field is reasonably circular.

(b) A measure of the variation of field intensity over this region.

The first measure is obtained by determining the area within which some prescribed axial ratio is maintained. A specific value was arbitrarily chosen to be 3db. This area is substantially an ellipse with one principal axis along the first axis of symmetry and the other transverse to it. The degree of uniformity was measured by determining the relative circular polarization constant at the termini of the principle axes.

It is only along the first symmetry axis that the symmetry and antisymmetry fields are perpendicular. Off this axis, these fields are oriented with respect to each

other at some angle ϕ. Equation (20) shows that the normal modes of the system are characterized by equal excitation of symmetric and antisymmetric incident energy in a quadrature phase relationship. If H_s and H_A are the resulting magnetic field amplitudes at some point in the cross-section, then relative to a cartesian frame oriented along H_s the vector field at that point is represented by

$$\left\| \begin{array}{c} H_s + iH_A\cos\phi \\ iH_A\sin\phi \end{array} \right\|$$

for one of the normal modes. The positive and negative circular polarization measures are given, respectively, by

$$\frac{1}{\sqrt{2}} \; (H_s - H_A\sin\phi + iH_A\cos\phi)$$

and

$$\frac{1}{\sqrt{2}} \; (H_s + H_A\sin\phi + iH_A\cos\phi)$$

The axial ratio is given by

$$A.R. = \frac{(H_s^2 + H_A^2 + 2H_sH_A\sin\phi)^{\frac{1}{2}} + (H_s^2 + H_A^2 - 2H_sH_A\sin\phi)^{\frac{1}{2}}}{(H_s^2 + H_A^2 + 2H_sH_A\sin\phi)^{\frac{1}{2}} - (H_s^2 + H_A^2 - 2H_sH_A\sin\phi)^{\frac{1}{2}}} \quad (25)$$

The difference in squared magnitudes between the two circular components is

$$\triangle C.P. = H_sH_A\sin\phi \quad\quad\quad\quad (26)$$

52

Employing equations (25) and (26), field plot
measurements were taken for the cross-sections shown in
Figures 10(b) and 10(c). The region of circular polari-
zation for the structure of Figure 10(a) was too narrow
for the field probe structure to be used accurately.
Figure 12 shows a summary of results for the symmetric
structure and Figure 13 provides similarly for the asym-
metric structure. Figure 14 shows the parallel strip
cross-section and indicates both the position of circular
polarization and the relative strength of C.P. excitation.

As indicated earlier, the asymmetric structure
seems the most efficient for a single ferrite rod, best-
ing the symmetric structure by the order of 60%. This
number derives from the calculation made for a ferrite
rod having the cross-section of the 3db axial ratio
ellipse and having a strength of circular polarization
excitation equal to that at the C.P. point. In actual
practice the ferrite area is at least an order of mag-
netude greater than that of the ellipse and the calculated
values shown in Figures 12 and 13 should be treated as
little more than relative indicators of performance.

Figure 14, included for completeness, indicates

53

$\Delta \beta$= .85 DEGREES / IN
FOR CROSS-HATCHED
AREA ONLY

.500

.094   .250

.081 D. TYP.

.500

CP POINT

$$\left(\frac{H^2}{P} = 1.35 \times 10^{-2} \frac{Mhos}{in^2} \right)$$

A
C
B
A

.019

.019

.014

.016

CP REGION AS
DEFINED BY 3db
AXIAL RATIO

$$\left(AREA = 8.96 \times 10^{-4} in^2 \right)$$
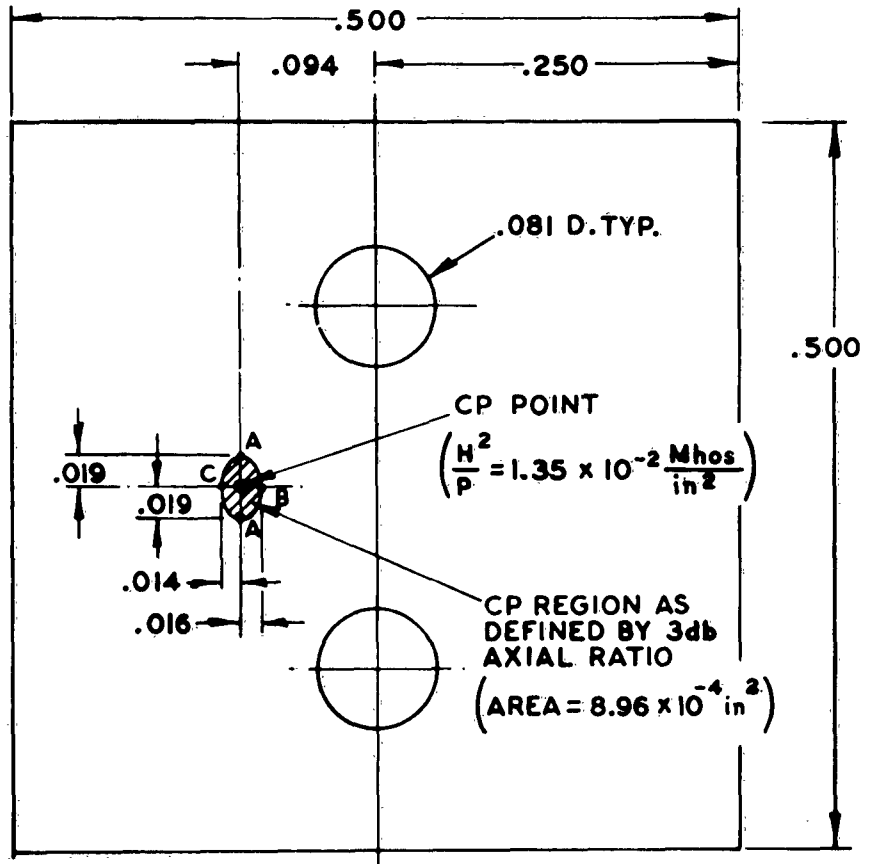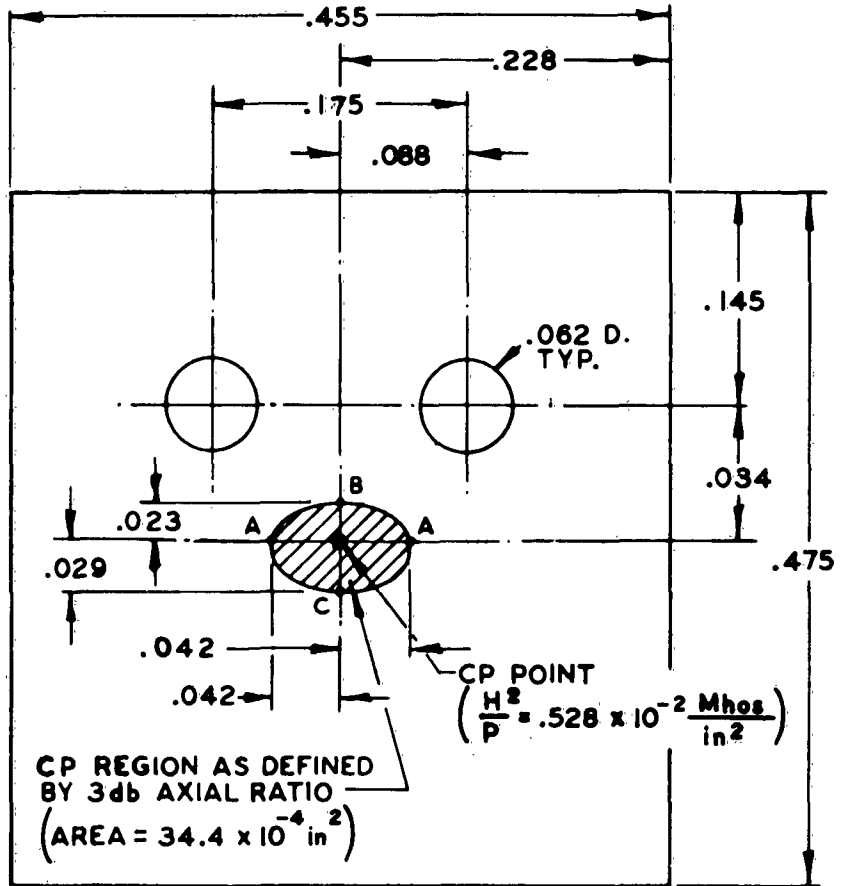
POINT	Δ C.P. IN MILLIMHOS / IN^2	% OF CENTER VALUE
A	10.1	74.8
B	20.0	148.3
C	8.7	64.8

FIGURE 12 – ELECTRIC FIELD DETERMINATIONS FOR
SYMMETRICALLY LOCATED ROUND
CONDUCTORS

54

FIGURE 13 — ELECTRIC FIELD DETERMINATIONS FOR SYMMETRICALLY LOCATED ROUND CONDUCTORS
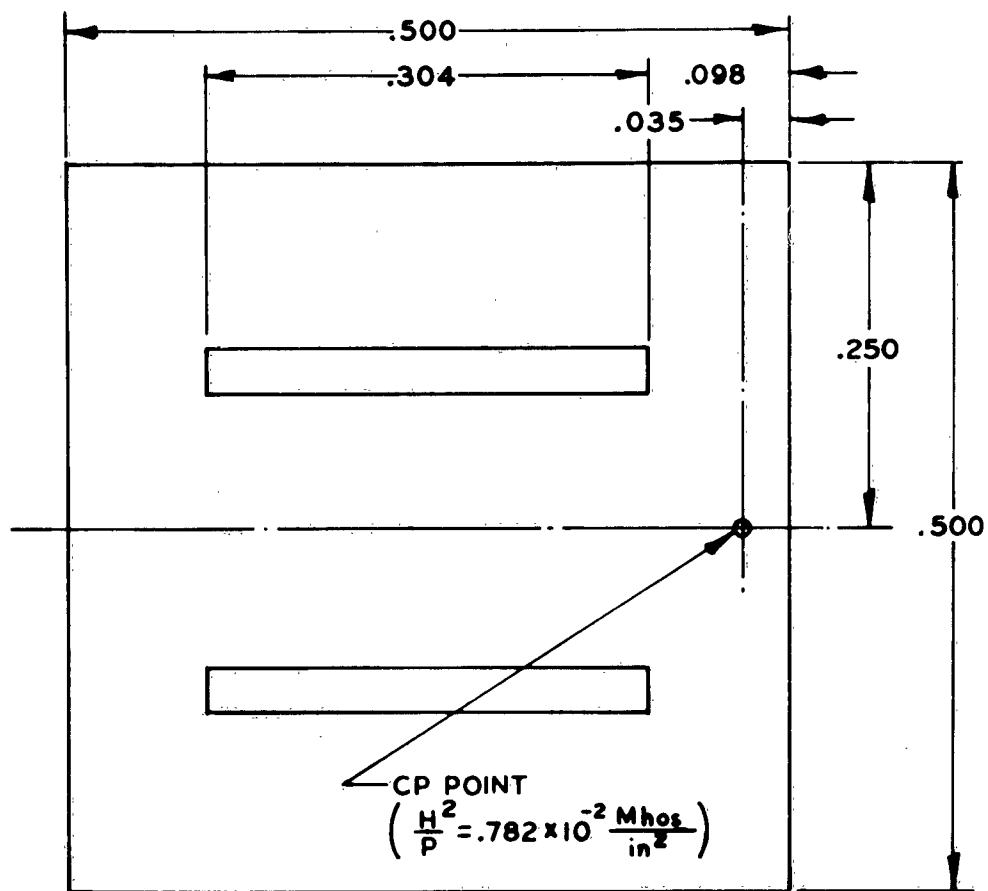
CP REGION IS MINUTE
BECAUSE OF CLOSE
PROXIMITY TO WALL

FIGURE 14 — ELECTRIC FIELD DETERMINATIONS FOR
STRIP CONDUCTORS

the unsuitability of the parallel strip structure for
the purposes intended here. It shows this structure to
have a circular polarization excitation greater than that
of the asymmetric structure and less than that of the sym-
metric, but its circular polarization area is so small as
to permit little integrated strength.

VI.   EXPERIMENTAL RESULTS

The construction of an extremely wideband non-reciprocal device is a study in compromise for the microwave designer. For broad bandwidth, the magnetization must be low since the minimum frequency is given by $\omega_{min} \cong 2\omega_m$. The ferrite rod may not be too large in cross-section or it will extend substantially out of the circular polarization area and provide for excessive loss. Further, a large cross-section increases the degree of dielectric inhomogeneity, requiring a greater precision of dielectric balance to offset forward coupling.

The combination of a small magnetization and a moderate cross-section makes for a small rotation rate and a very long and slender ferrite rod. The support of this long structure demands the use of an adequate number of beads, randomly spaced to minimize reflection over the large bandwidth. The dielectric compensation requirement is simplified by the use of several cascaded ferrite rod sections, where each rod portion is individually adjusted for compensation. These sections are each tapered to minimize reflections.

The conductors themselves are tapered from the

58

input fittings to avoid backward wave coupling effects as discussed in Section II. The combination of conductor tapers, ferrite tapers, the multiplicity of beads, the fitting mismatches themselves, etc., conspire to produce disquietingly large reflections. A circulator, as is evident, is critically susceptible to reflection effects and design requirements are stringent to reduce them to minimal values.

The above description of the experimental difficulties of the construction of the circulator comes as the result of the study of three test models which, essentially, constituted the experimental study program. Two types of cross-section were studied; strip line and circular rod center conductors. The first two models were built in strip line and they are shown in Figures 15 and 17. The last model contained the circular rod geometry and is shown in Figure 21. All the structures used the Kearfott AN 50 material whose characteristics are discussed in Section IV of this report.

The first test structure, that of Figure 15, has a ferrite rod length of roughly 6.5", effectively, taking taper volume into account, and a square cross-section of
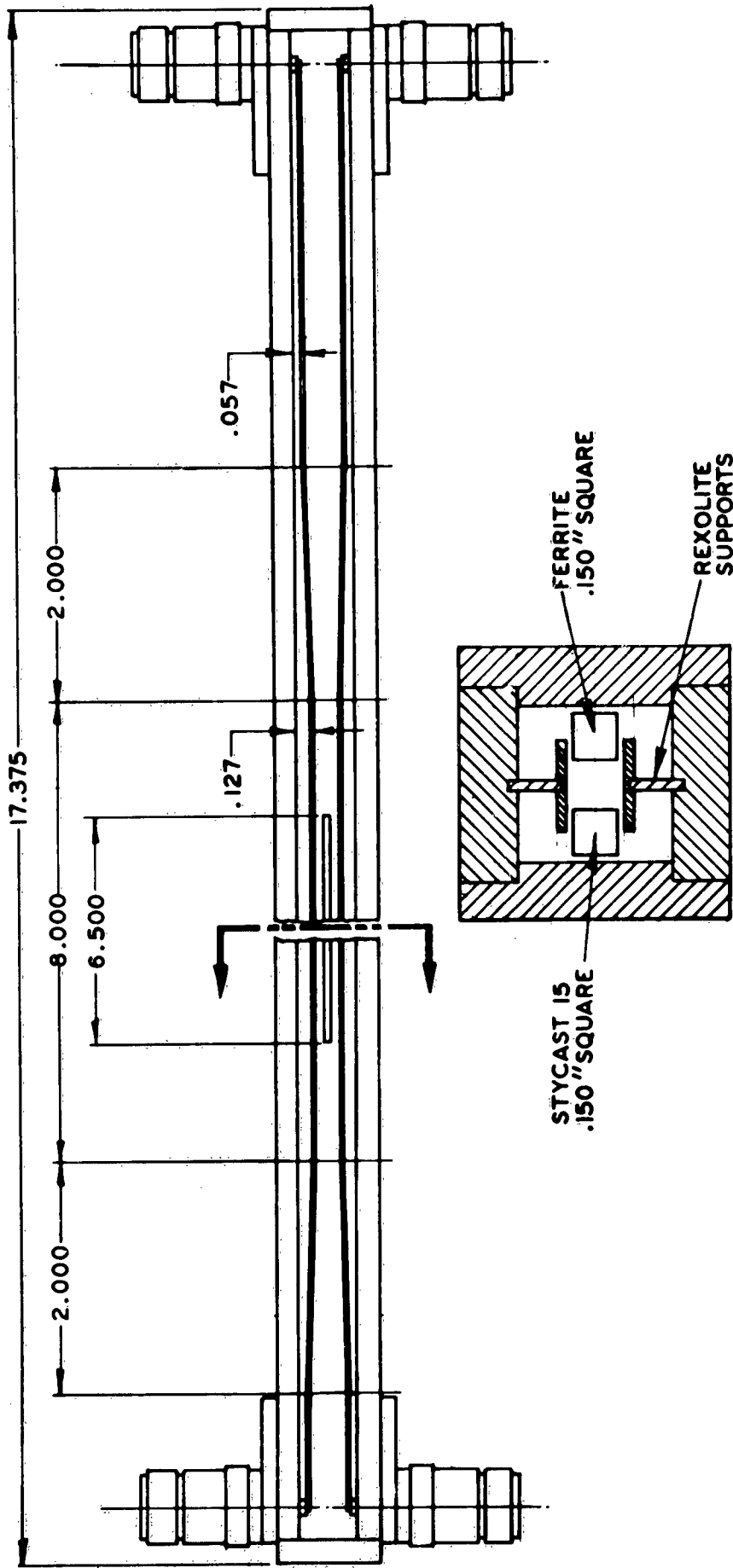
FIGURE 15—FIRST TEST MODEL

17.375

2.000

.057

2.000

8.000

6.500

.127

FERRITE
.150" SQUARE

REXOLITE
SUPPORTS

STYCAST 15
.150" SQUARE

60

.150" on a side. Figure 16 shows that the backward coup-
ling undulates rapidly over large values in the unmag-
netized state whereas the forward coupling is relatively
smooth. This would tend to indicate that backward coup-
ling occurs through the reflections of the inadequately
matched strip line tapers while forward coupling takes
place through remanent magnetic effects of the ferrite
due to imperfect cancellation within the domain structure
of the material.

A 50 oersted field essentially completely sat-
urates the ferrite. The forward coupling is again uni-
form with an increase in value of approximately 10db,
producing a value of θ of about 10° at 2.5 kmc. It is to
be recalled that a value of 90° is required for θ to pro-
duce a circulator.

Most interesting of the experimental results is
the fair degree of flatness of θ over a large frequency
range, showing that a Faraday rotation indeed takes place.
Were the coupling primarily dielectric rather than mag-
netic in nature, the transmission would be sinusoidal over
the band observed. The computed coupling runs about 50%
higher than that observed but, considering the great

61
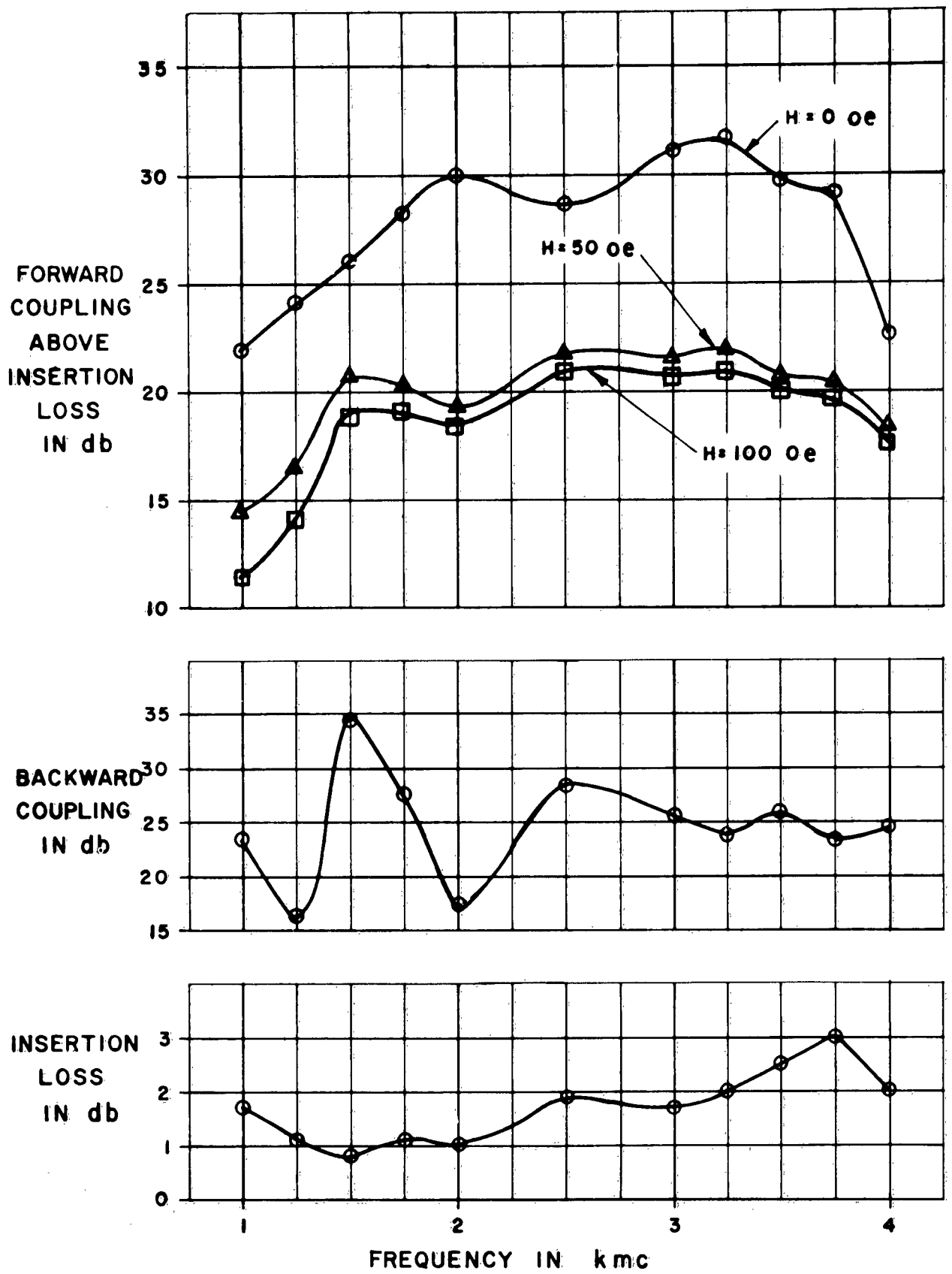
FIGURE 16 – PERFORMANCE CHARACTERISTICS
OF FIRST MODEL

62

roughness of the perturbation assumptions and the questionable applicability of a demagnetizing formulation, the correlation of experiment to theory is more than adequate.

The correlation of experiment to theory is even further clouded by the fact that the magnetic coupling is small and significant error oould occur in the presence of dielectric coupling. Nevertheless, the results of the first model were employed as a basis for constructing a second which, it was hoped, would provide the requisite 90° rotation. As shown in Figure 17, a $26''$ long strip line structure was built with the $.150''$ square ferrite loading both sides of the strip cross-section. Longitudinally magnetized Alnico bar magnets were attached, oppositely polarized, to the walls of the outer conductor with the intention of saturating the two ferrite rods in opposed directions. Unfortunately, the spacing of the magnets to the ferrite was too large and the magnets tended to act more as keepers for one another than to supply ample field to saturate the ferrite rods.

Had time proved adequate, the bar magnets might have been incorporated into the outer conductor with the

63
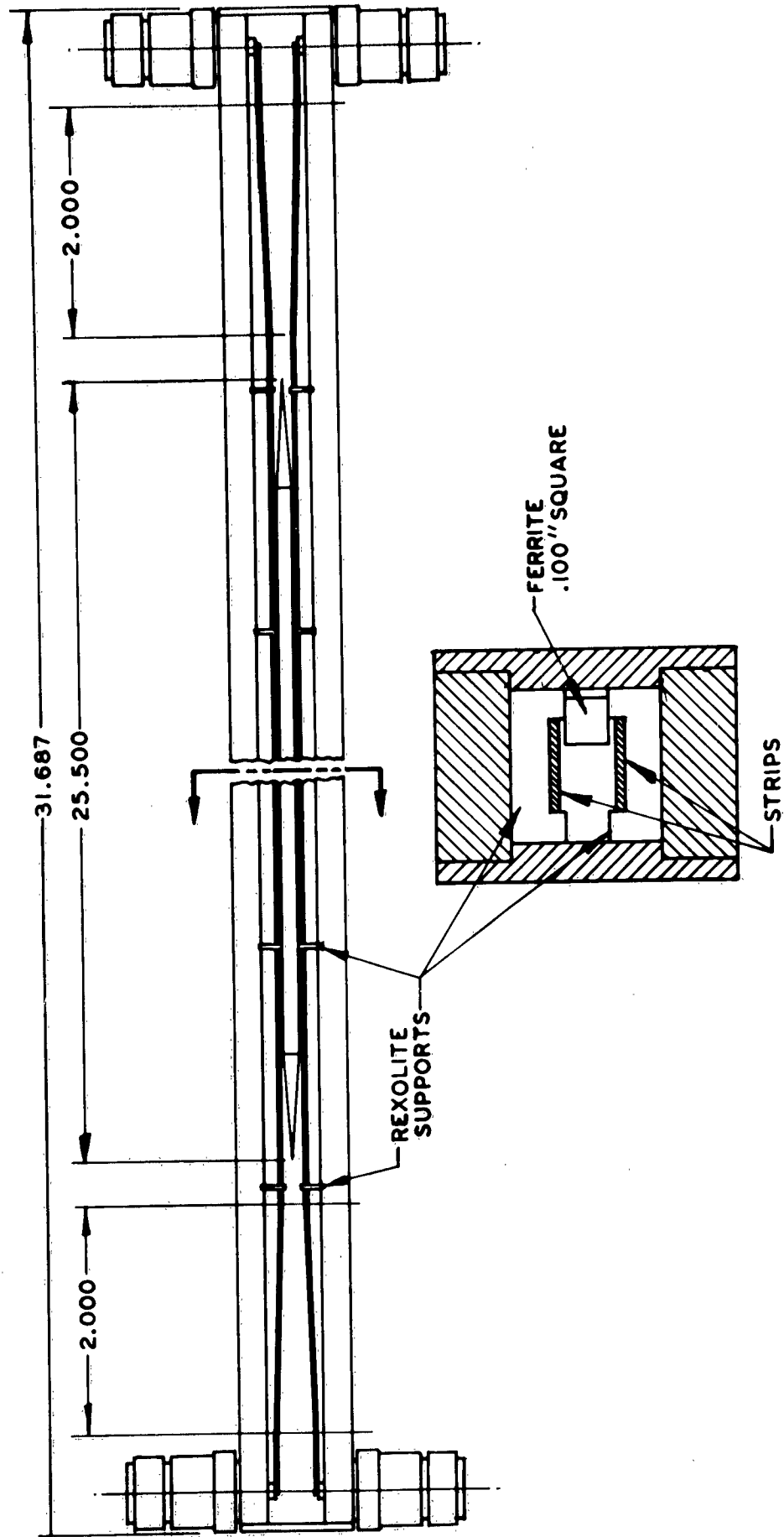
FIGURE 17 — SECOND TEST MODEL

FERRITE
.100'' SQUARE

STRIPS

REXOLITE
SUPPORTS

31.687

25.500

2.000

2.000

64

structure operating in the intended fashion. As it was, one ferrite member was removed, and replaced by a dielectric rod which operated as a dielectric coupling vernier. A single turn solenoid was then constructed over the 26" length to provide the unidirectional field now required.

Since the second model was quadruple the length of the first, a value of θ of 40° was anticipated, calculating to an 11.4db increase in coupling over the first model. The data of Figure 18 show an actual increase of about 10db over the first model, reasonably vindicating the results of that unit. Figure 18 shows the forward coupling to vary to a much greater degree than acceptable. The cause of the variation was ultimately traced to the periodicity of the beads used to support the large span of the strip inner conductors, which created large reflections for constructive interference. It is of interest to note that the backward coupling, in this case, is also a function of field, unlike the results of the first unit. The degree of Faraday rotation is larger in the 26" unit and reflection with Faraday rotation combined with backward coupling effects produces the complex field sensitive

65

FORWARD COUPLING IN db

H = 0 oe

H = 50 oe

BACKWARD COUPLING IN db

INSERTION LOSS IN db

FREQUENCY IN kmc
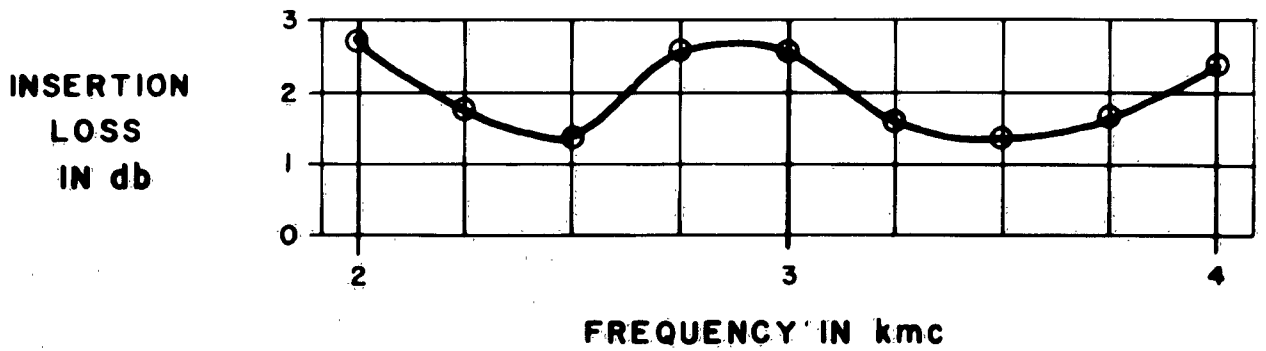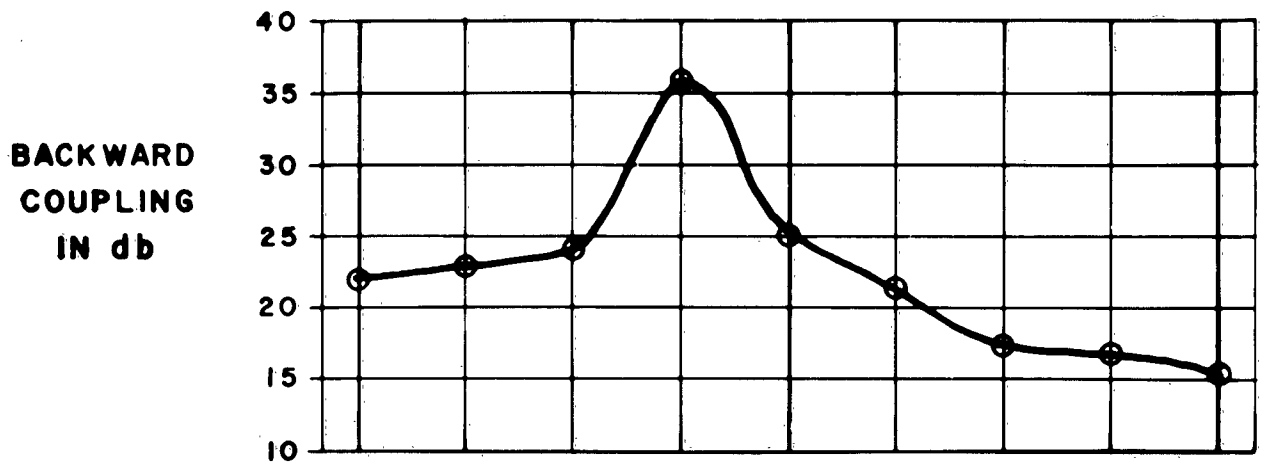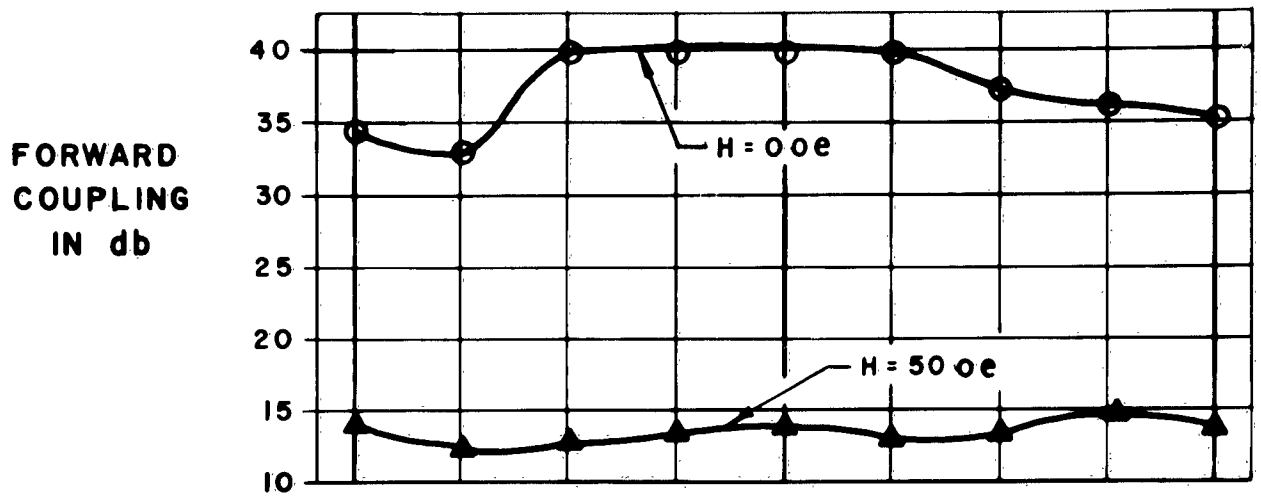
FIGURE 18 — PERFORMANCE CHARACTERISTICS
OF SECOND MODEL

66

interferences observed.

An alternative construction to that employing periodic bead loading was that using a thin tapered dielectric web to support the strip line center conductors along their entire length. The electrical characteristics are shown in Figure 19 where, it is observed, the dielectric tends to produce dispersion in the coupling. Not only is the rotation rate frequency sensitive, but is greater at all frequencies than that for air loading.

Any attempt to reduce the width of the web leads to making the structure excessively fragile. The ultimately desired extreme to the inhomogeneous loading, namely complete loading with dielectric material, could not be employed because of the severe experimental problems of dielectric adjustment of the ferrite member. Dielectric coupling may be entirely mitigated by embedding the ferrite in a medium of identical dielectric constant but this, it was felt, would lead to excessive loss and moding difficulties which would not be resolved within the remaining time of the contract.

It was decided, finally, to support the strips with very thin dielectric supports, randomly spaced, and

67
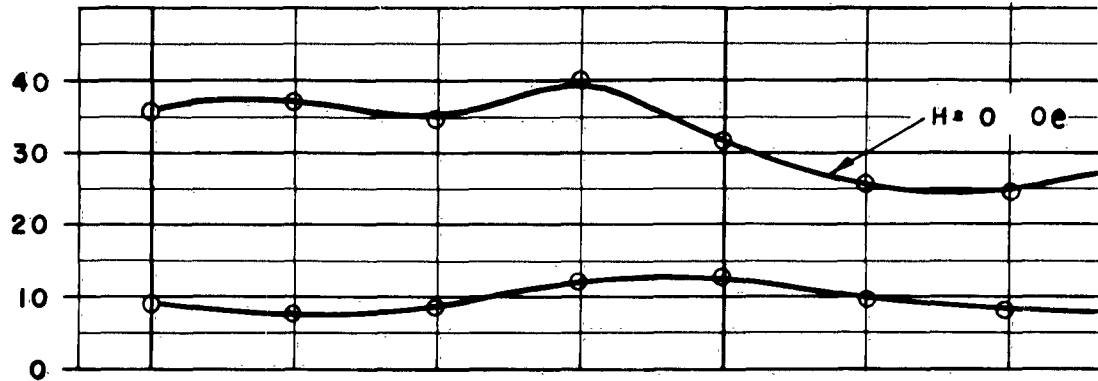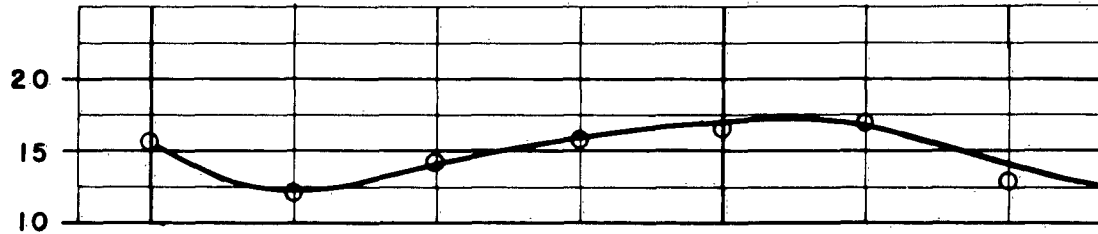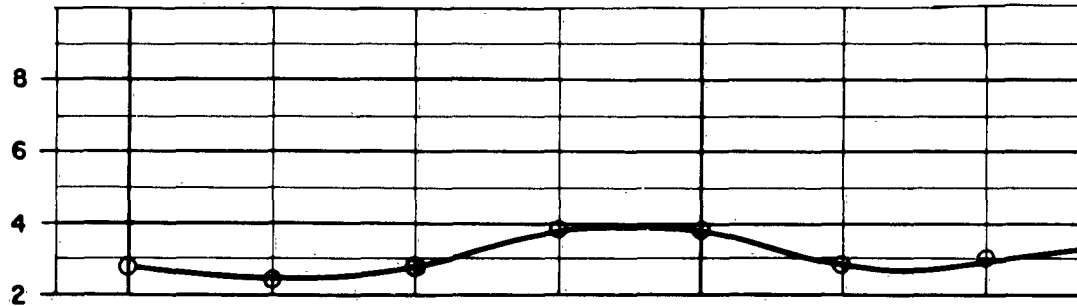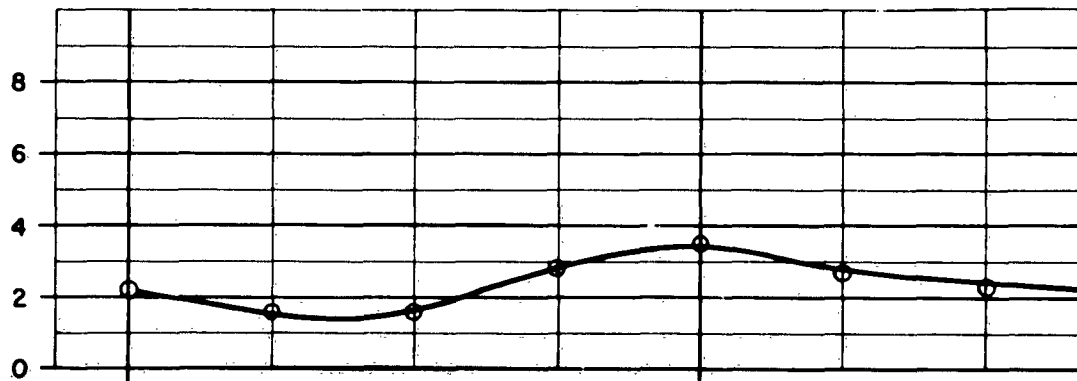
FIGURE 19 - PERFORMANCE CHARACTER
SECOND MODEL FIRST M

H= 0 0e

H= 50 0e

FREQUENCY IN kmc

19 – PERFORMANCE   CHARACTERISTICS OF
SECOND MODEL   FIRST MODIFICATION

2

to remove the vernier dielectric rod used for dielectric compensation, to free the cross-section of excess dielectric material. In attempting to make the ferrite member self compensating, it was found that the compensation condition on the centroid was closer to the wall than the ferrite could be moved physically. It was then necessary to reduce the ferrite cross-section, and a new ferrite dimension was chosen of .100" on a side. Performance is shown in Figure 20 which demonstrates a small backward wave coupling over a large frequency range and a flat forward coupling of 21db over the same range.

The difficulties encountered in the strip line structure in terms of both small rotation rates and the self compensation of a moderate ferrite cross-section made it desirable to seek out another cross-section. The cross-section chosen was that of the Stanford Research Institute[*] and for which successful isolator operation had been achieved at much higher frequencies. It is shown in Figure 10C and is composed of a pair of off center circular rod conductors in a rectangular outer conductor housing. The actual device is shown in Figure 21. It is a U shaped structure magnetized by a coextensive

*E.M.T. Jones, G.L. Matthei, and S.B. Cohn, "A nonreciprocal, TEM-Mode structure for wide-band gyrator and isolator applications," IRE Trans. on Microwave Theory and Techniques, vol. MTT-7, pp. 453-460; October, 1959.

FORWARD
COUPLING
ABOVE
INSERTION
LOSS IN db

35
30
25
20
15

H = 60 Oe

BACKWARD
COUPLING
IN db

40
30
20
10

INSERTION
LOSS
IN db

3
2
1
0

VSWR

3.0
2.5
2.0
1.5
1.0

1   2

FR

1
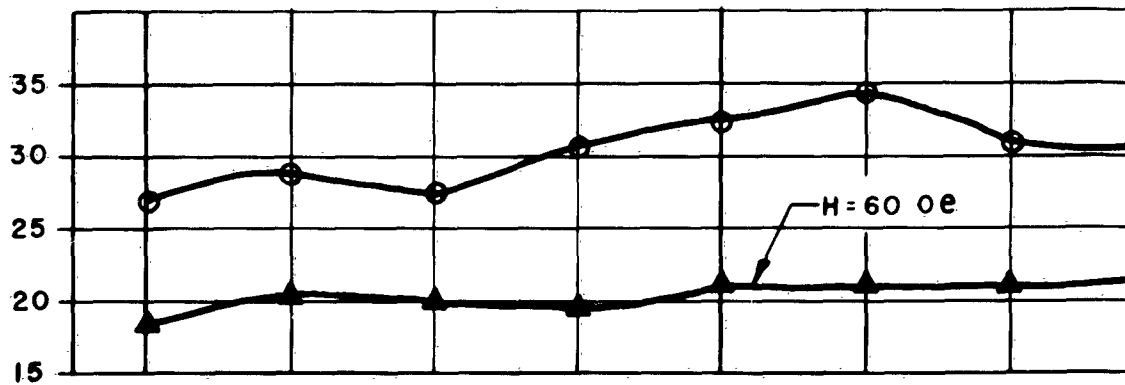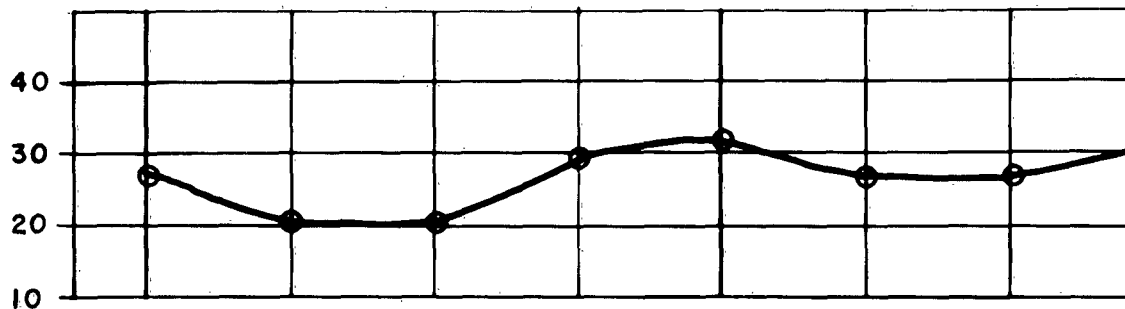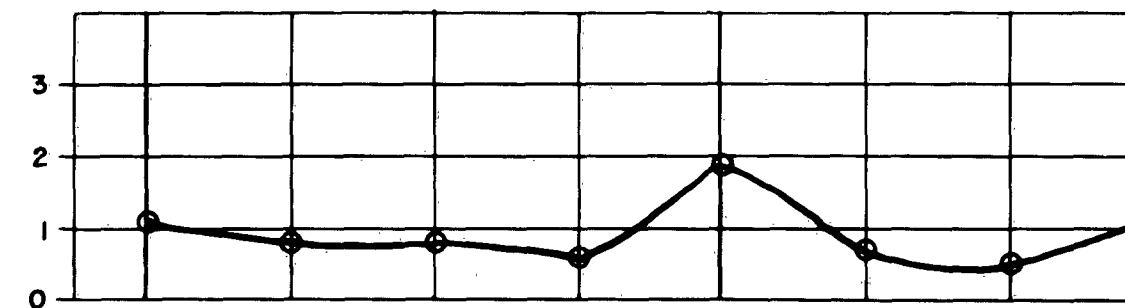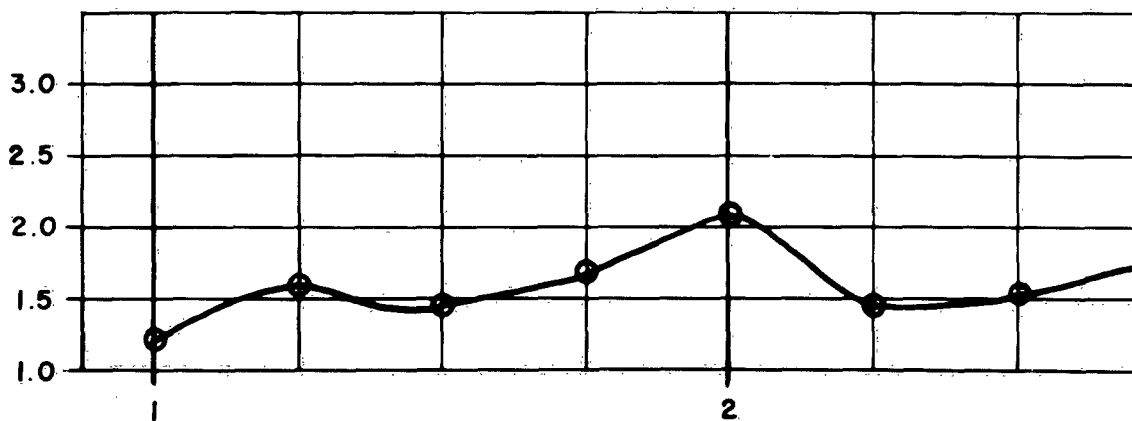
FIGURE 20 - PERFORMANCE CHARACTERIS
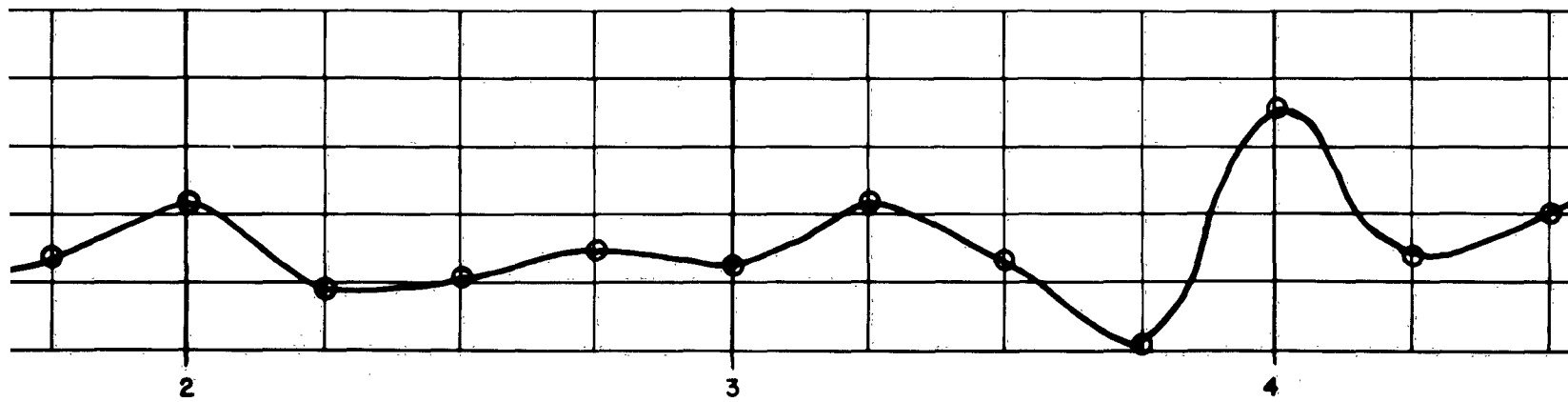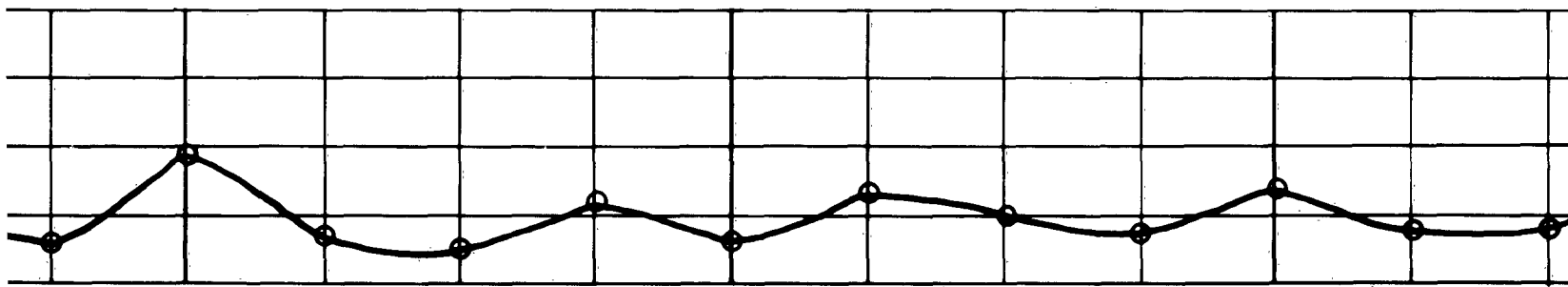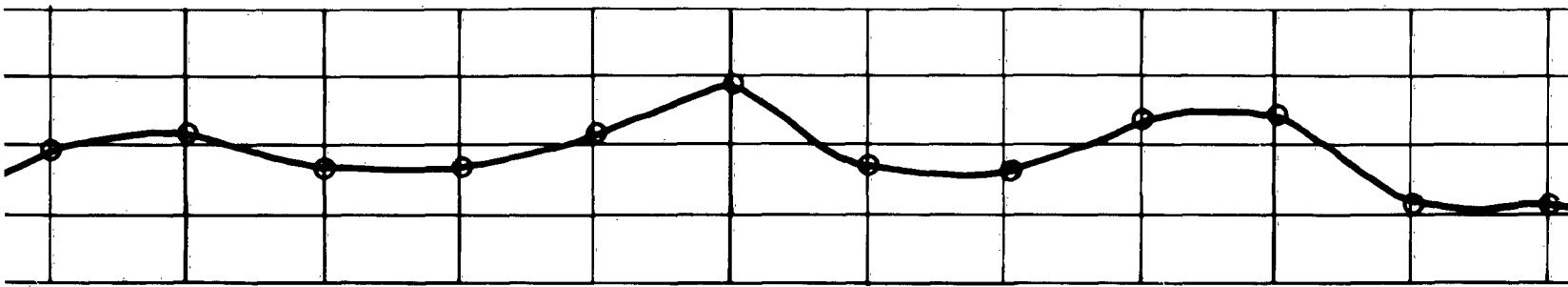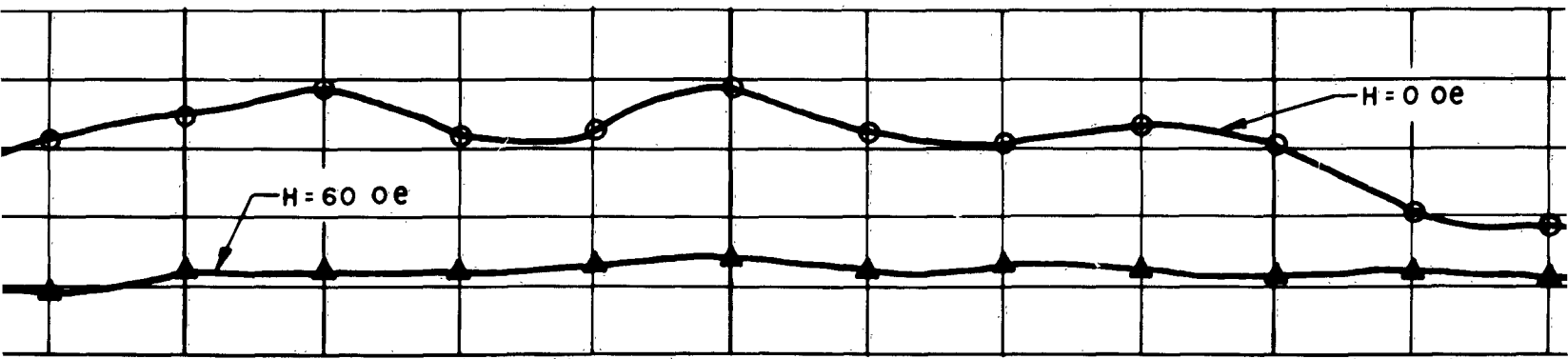
H=0 oe

H=60 oe

FREQUENCY IN kmc

O-PERFORMANCE CHARACTERISTICS OF SECOND MODEL SECOND MODI[

2

H = 0 oe
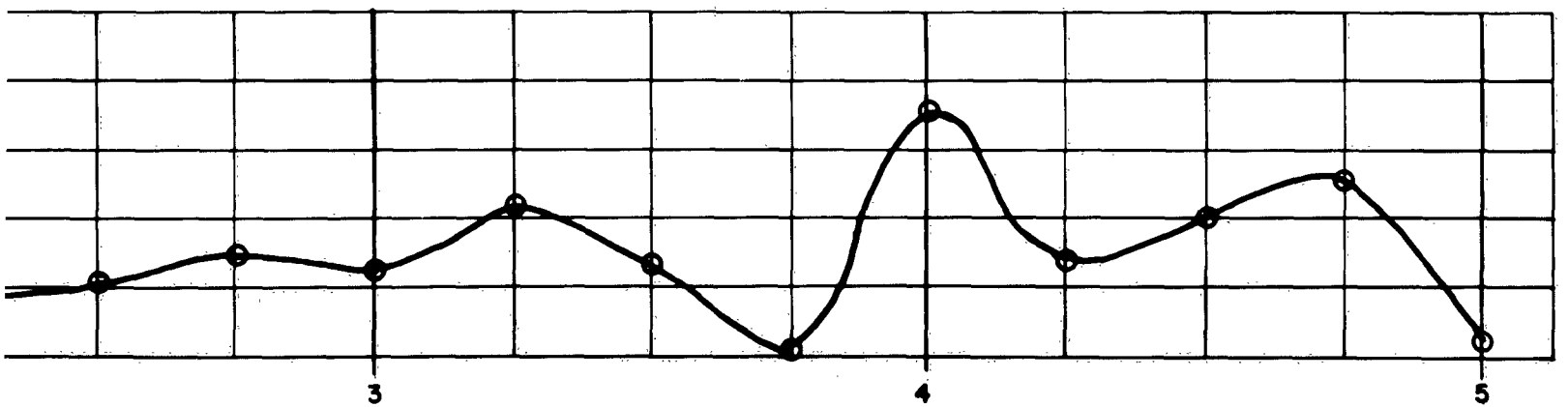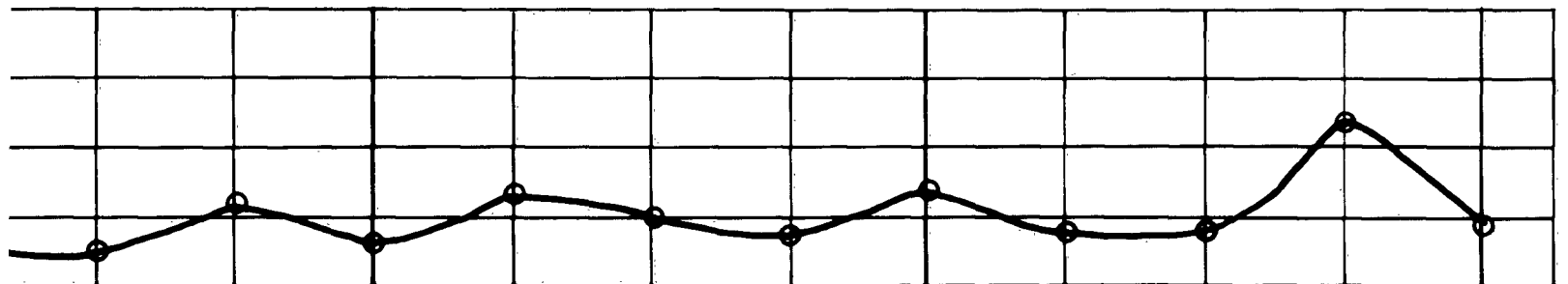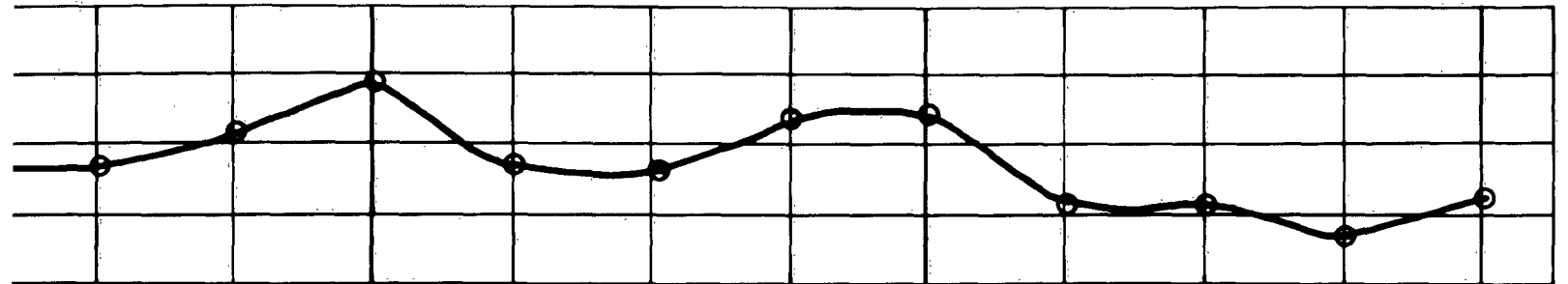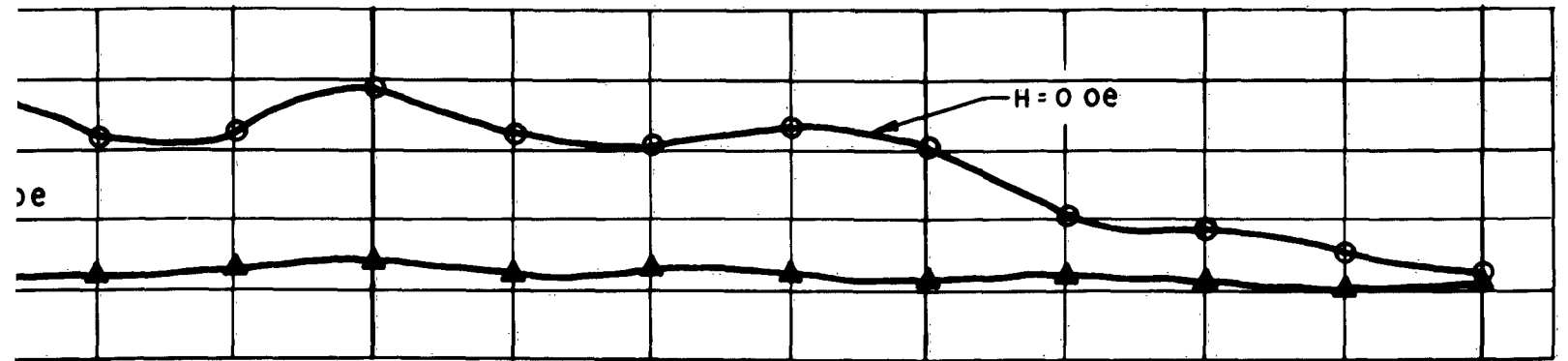
FREQUENCY IN kmc

CHARACTERISTICS OF SECOND MODEL SECOND MODIFICATION

3

70

11.250 T

35.875

9.000

REXOLITE
SUPPORTS

CONDUCTORS

FIGURE 21—FINAL TEST

1

11.250 TYP.

35.875

.ITE
RTS

RS

FERRITE
.160" SQUARE
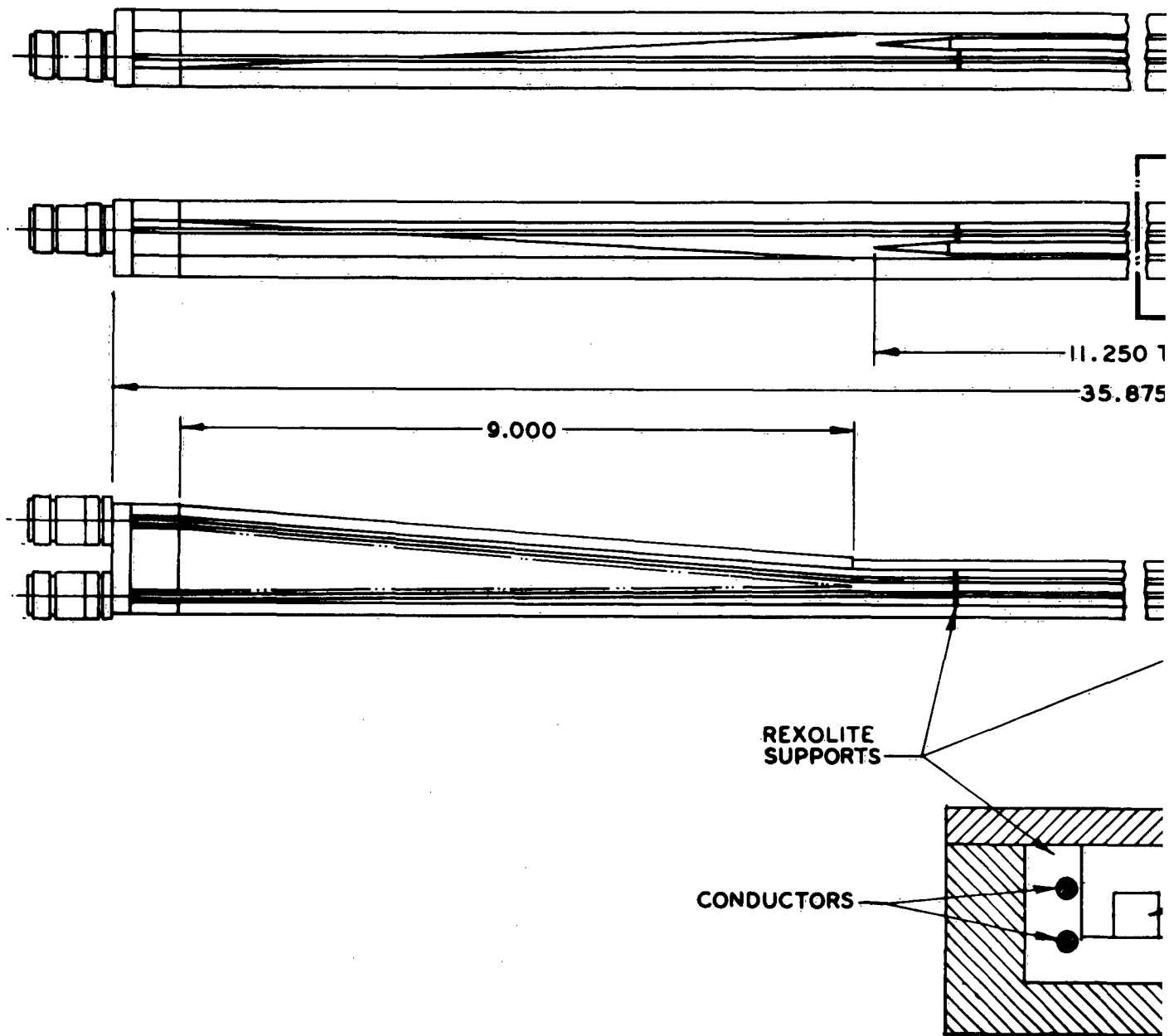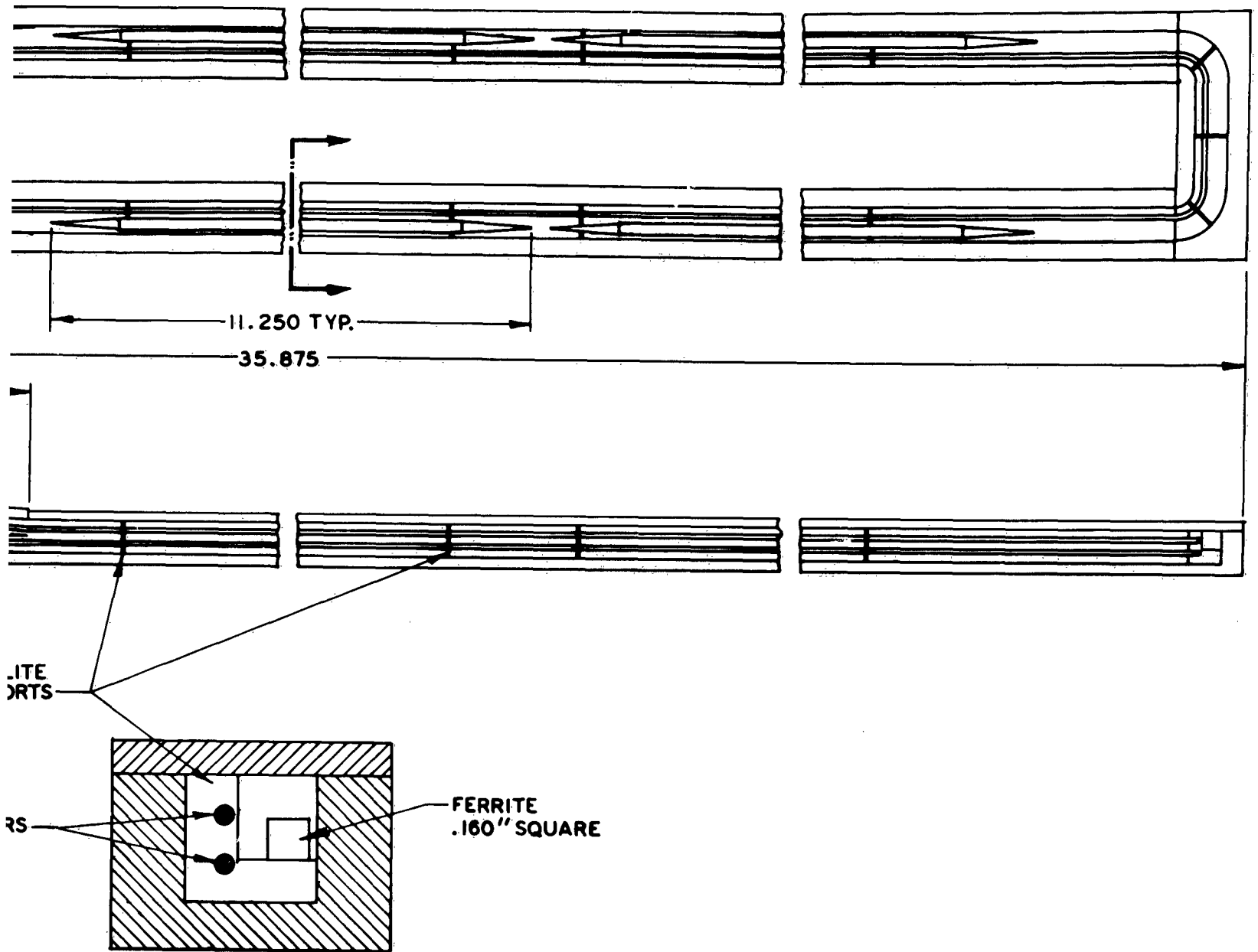
FIGURE 21—FINAL TEST MODEL

71

2

FORWARD COUPLING IN db

H = 0 oe

H = 100 oe
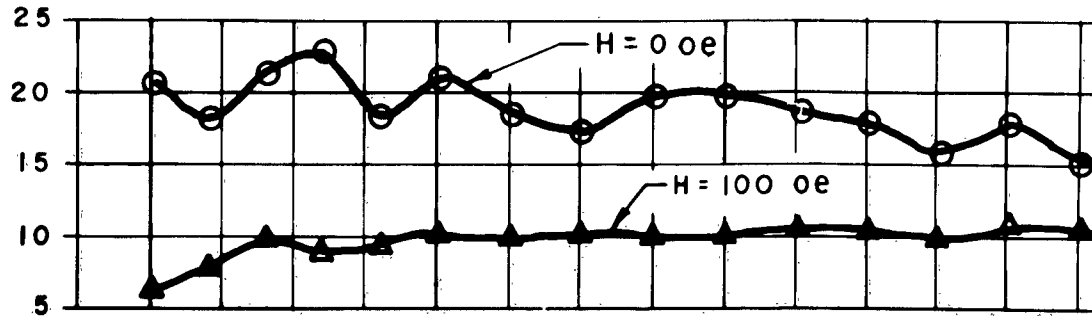
BACKWARD COUPLING IN db
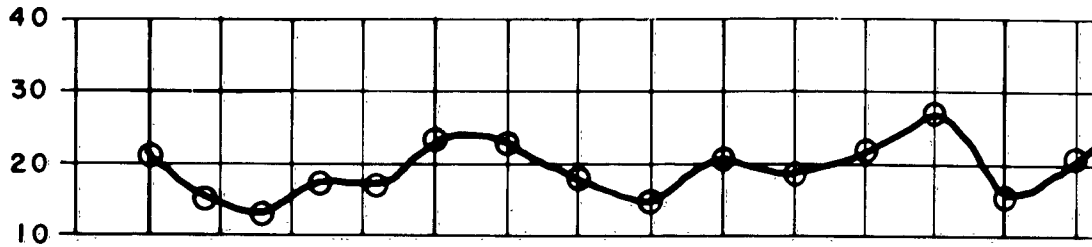
INSERTION LOSS IN db
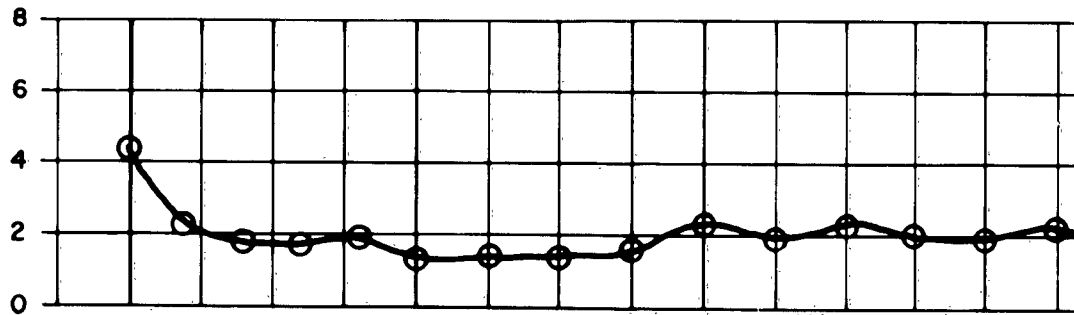
VSWR
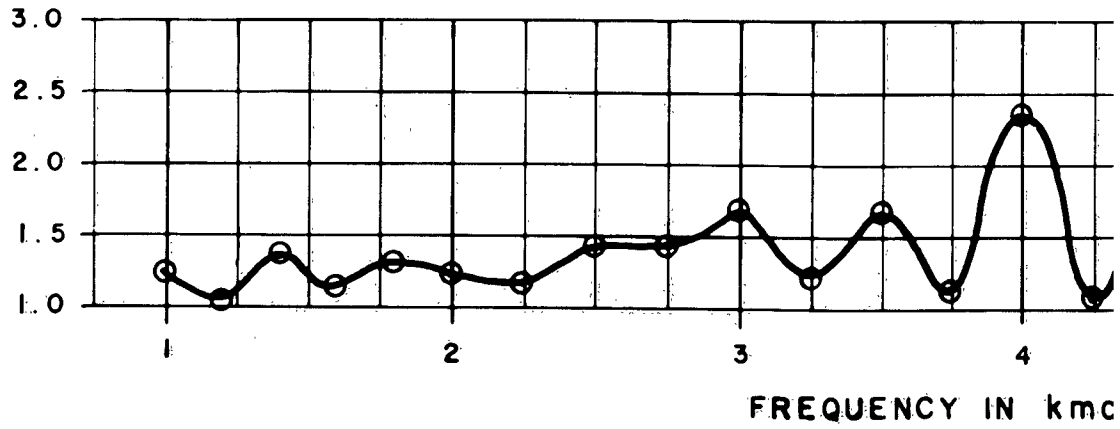
FREQUENCY IN kmc

FIGURE 22 – PERFORMANCE CHARACTERISTICS OF
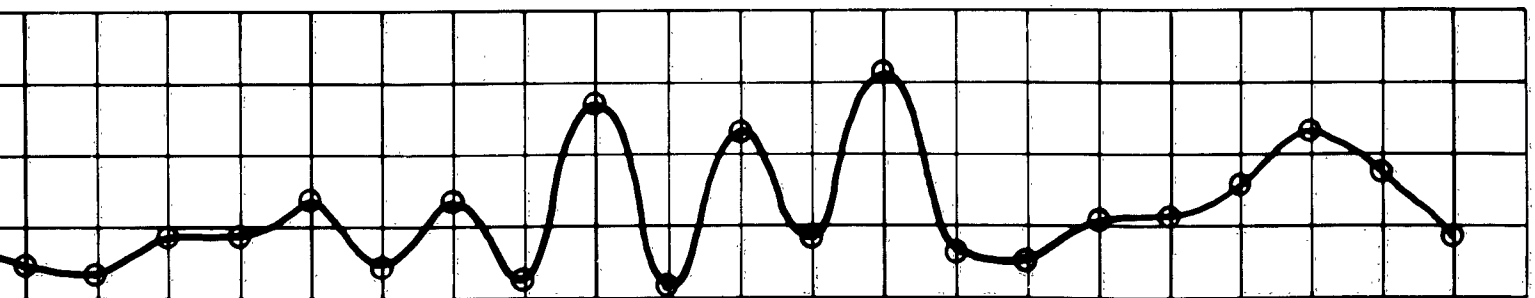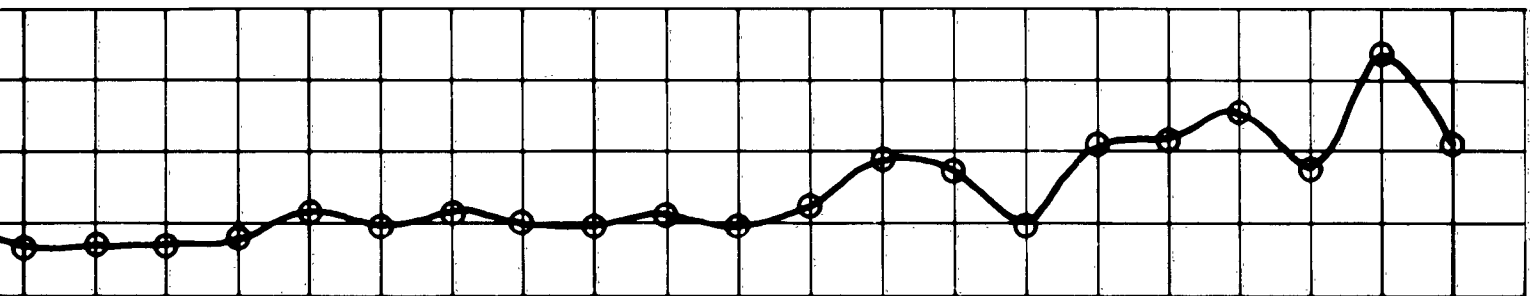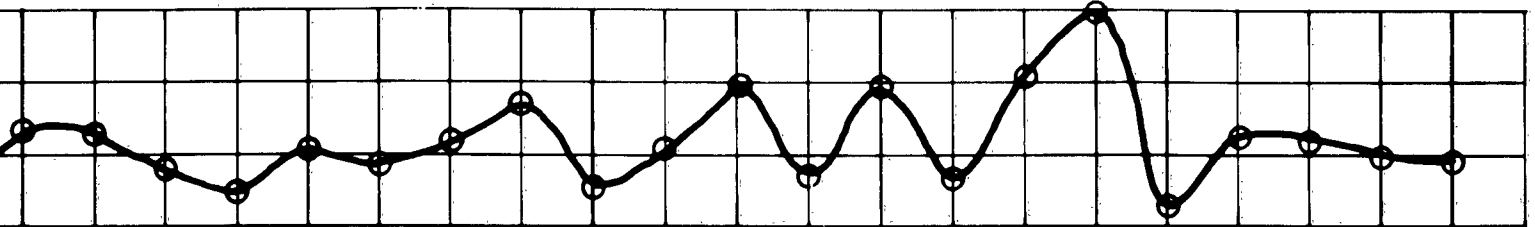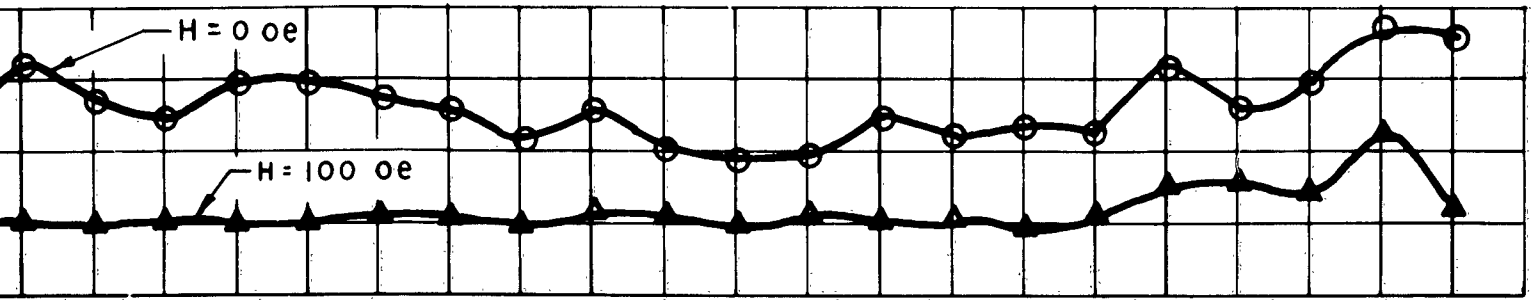
FREQUENCY IN kmc

FORMANCE CHARACTERISTICS OF FINAL MODEL

72

2

single/layer solenoid, containing an effective 41" length of .160" square AN-50 ferrite.

The coupling characteristics are shown in Figure 22. The major quantity of interest is the forward coupling which shows a substantially constant 10db value, inclusive of losses, from 1.8 to 5.6 kmc. The coupling corresponds to a value of θ of about 36° which is a factor of two under calculation for this structure.

Backward coupling is observed as a severe problem over the frequency range for several reasons.

1) The tapers are inadequately matched at the the low frequency end

2) The guide distortion at the terminals to accomodate the tapers leads to higher moding at the high end.

3) The U bend leads to reflections in the mid and upper frequency ranges.

These results are seen also in the VSWR characteristic which show structural difficulties beyond 4 kmc.

Figure 23 carries the forward coupling curve down to very low frequency ranges as a matter of interest. A broad resonance is observed at 900Mc with a 60 oersted

73
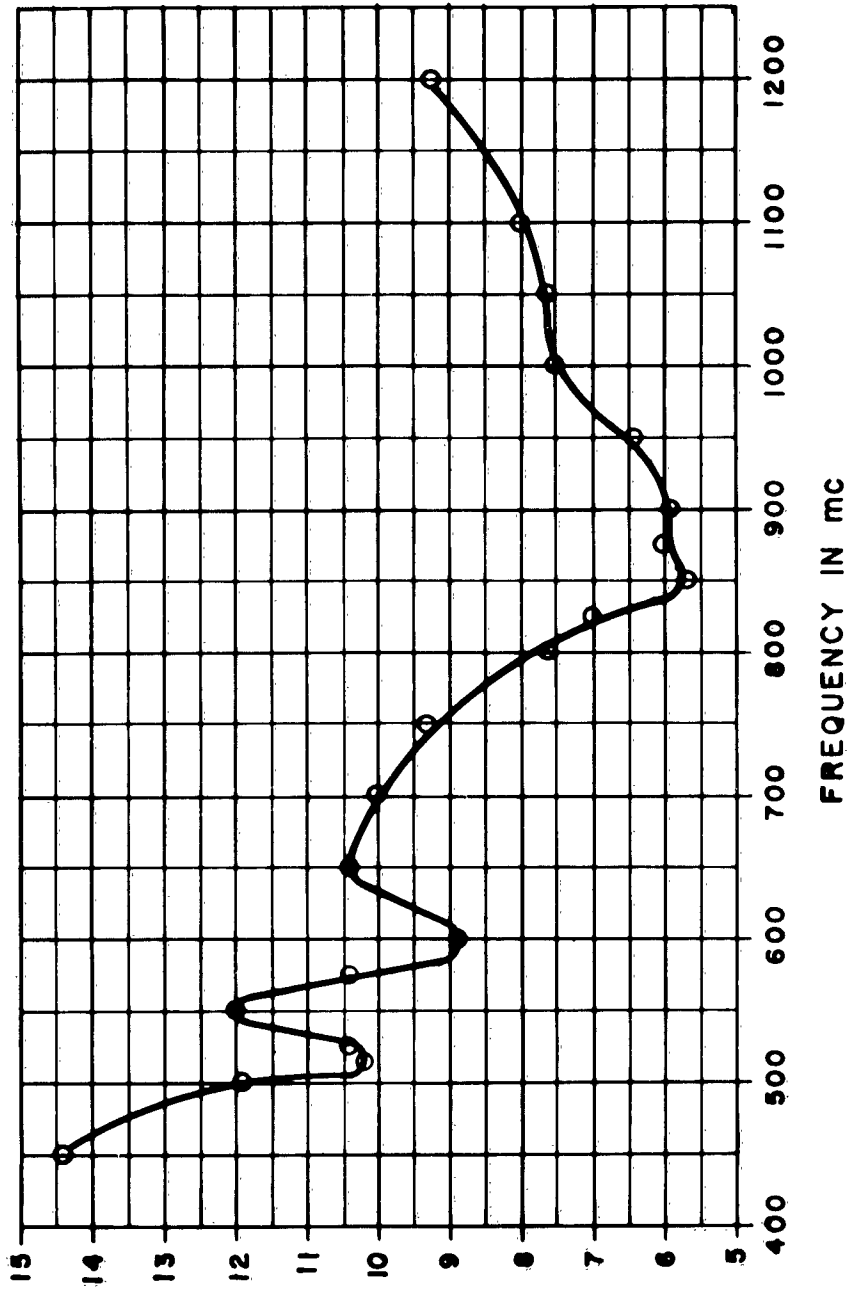
FORWARD COUPLING IN db

FREQUENCY IN mc

FIGURE 23 - COUPLING OF FINAL MODEL AT LOW FREQUENCIES

applied field. Below this frequency, the coupling diminishes, with interference effects produced by terminal reflections clearly visible on the curves.

It was of interest, from the point of view of both establishing the degree of saturation of the ferrite and the demonstration of broad band variable directional coupling principles to explore this structure along the ferrite saturation curve. Figure 24 explores rotational coupling as a function of magnetic field at 2, and 3, and 4 kmc respectively. The couplings vary quickly with low fields coming to saturation at roughly 40 oersteds. There is trivial difference between the various curves, with the slight differences accountable to either dielectric or backward wave coupling. As is to be expected, these effects are most clearly accentuated on the 4 kmc characteristic.

The failure to achieve a 90° value for Θ was disappointing based on the SRI isolator results. There, with a substantially identical cross-section and with approximately 4 times the magnetization a value of 90° was achieved in roughly 1/7 the length. This tends to argue four times the structural efficiency of the circulator with a fourfold increase of the magnetization. The computations of
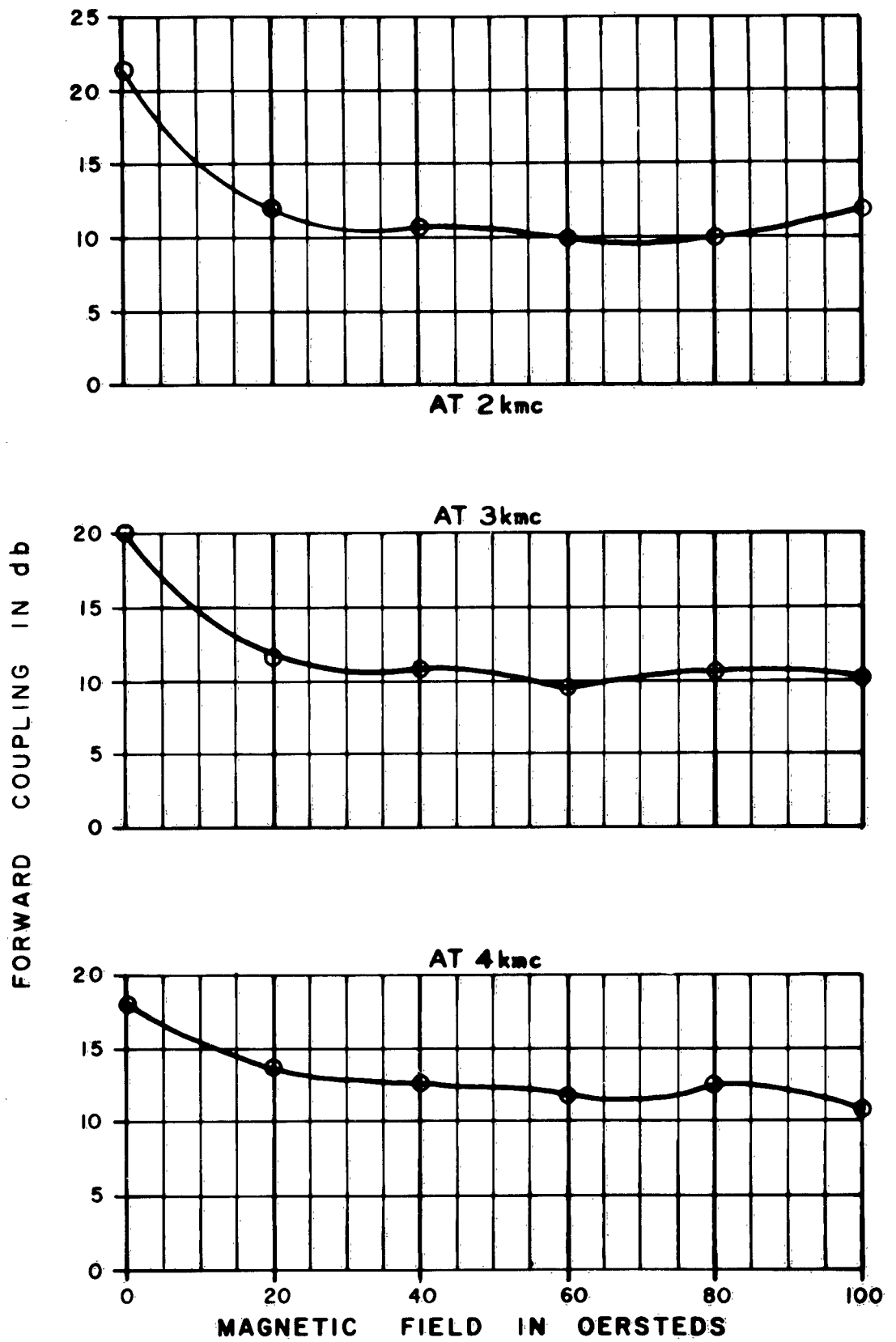
FIGURE 24- FORWARD COUPLING vs
MAGNETIC FIELD FOR
FINAL MODEL

this report admittedly accepted a rather crude basis of approximation and presumed a linear relation of rotation rate to magnetization. With the conflicting results employing widely different magnetization values, it appears that a linear magnetization theory is grossly inadequate.

Because of the severity of these conclusions, it was deemed necessary to conduct an experiment using General Ceramics R-1 ferrite as was done by SRI. A test was performed at 6 kmc using the device as a three arm circulator. The circulator operated effectively and at a ferrite length prescribed by the SRI isolator result. Thus, two demonstrations were made in this test:

1) Rotation rate is not a linear function of magnetization

2) The nonreciprocal principles proposed by this report are correct.

VII CONCLUSIONS

It has been demonstrated that broad band Faraday rotation effects can be observed in a gyromagnetically coupled two wire coupled line. Many basic nonreciprocal, as well as reciprocal devices emanate from this structure including circulators, isolators, gyrators, modulators, baluns, directional couplers, etc. All of these devices possess, in principle, the bandwidth of the basic structure.

The major difficulty in realizing this structure for extreme bandwidth is that of the very size of the device made ponderous by its need for a weak rotation rate. The device becomes lossy through its excessive length and the internal structure supports become the basis for unwanted dielectric coupling.

The avoidance of backward wave coupling effects was shown to require a tapering of the inner conductors from a region of substantially no coupling to one of intimate coupling between conductors. Since this cannot be done as a constant impedance transition for both even and odd modes similtaneously, very long tapers are required for operation including a low frequency range.

The flatness of Faraday rotation in a two wire line has been amply demonstrated. However, in a typical structure examined, with good response between 1.8 and 5.6 kmc, a structural length of about 100" would be required to form a circulator in an air dielectric coupled line. Examination shows, however, that the coupling rate is, to first order, proportional to the square root of the dielectric constant for a constant cross-section. Embedding the ferrite in a medium equal to its own dielectric constant would not only diminish dielectric coupling, but would diminish the structural length by a very significant factor.

For all its design difficulties, the twin conductor ferrite structure looks most promising for device application. A single frequency 6 kmc circulator was built showing its principles to be sound. More intensive studies of optimum conductor cross-sections and the use of antisymmetrically magnetized double ferrite rod cross-sections should significantly improve on the coupling rate problem with a corollary effect on structure size. This, together with dielectric loading, should make for a sturdy, compact device, having most attractive characteristics and versatility.

79